Insights on the evolution of vertebrate microbiomes from the analysis of the Xenopus frog microbiota across life stages.

Thibault Scalvenzi, Isabelle Clavereau and Nicolas Pollet*

Evolution, Génomes, Comportement & Ecologie, Université Paris-Saclay, CNRS, IRD, 91198 Gif-sur-Yvette, France

*Corresponding author:

Nicolas Pollet
Laboratoire Evolution, Génomes, Comportement et Ecologie
CNRS
1 Avenue de la Terrasse
Batiment 13
F-91198 Gif-sur-Yvette
France
Tel: 33 01 69 82 37 10
Fax: 33 01 69 82 37 36

Abstract (350 words max)

Background: The microorganism world living in amphibians is still largely under-represented and under-studied in the literature. Among anuran amphibians, African clawed frogs of the *Xenopus* genus stand as well-characterized models with an in-depth knowledge of their developmental biological processes including their metamorphosis. We used different approaches including flow cytometry, 16s rDNA gene metabarcoding, metagenomic and metatranscriptomic to analyze the succession of microbial communities and their activities across different body habitats of *Xenopus tropicalis*.

Results: We analyzed the bacterial components of the *Xenopus* gut microbiota, the adult gut biogeography, the succession of communities during ontogeny, the impact of the alimentation

in shaping the tadpole's gut bacterial communities, the transmission of skin and fecal bacteria to the eggs. We also identified the most active gut bacteria and their metabolic contribution to the tadpole physiology and showed the close resemblance between amphibian and mammalian gut microbiomes.

Our results show that in the growing tadpole, the same predominant bacterial phylum as in the mammalian gut is present as a large fraction of the 82,679 genes identified in the *Xenopus* tadpole's gut metagenome encode proteins sharing common functions with proteins found in the human gut microbiome.

Conclusions: We present a comprehensive new microbiome dataset of a laboratory amphibian model. Our data provide evidences that studies on the *Xenopus* tadpole model can shed light on the interactions between a vertebrate host and its microbiome. We interpreted our findings in light of bile acids being key molecular components regulating the gut microbiome composition during amphibian development and metamorphosis.

Keywords (3-10): Xenopus, Amphibian, Microbiome; Metamorphosis, Metagenome; Metatranscriptome

Background

Metazoans are vehicles for microbial communities, also named microbiota. The microbiota and its metazoan host have mutualistic interactions and are thought to adapt and evolve as holobiont (Wilson and Sober, 1989; Gill *et al*., 2006; Zilber-Rosenberg and Rosenberg, 2008; Bordenstein and Theis, 2015). Several studies have highlighted the importance of the microbiota in the function and development of several organs such as the alimentary canal, the nervous system and the tegument ...) (Sekirov *et al*., 2010; Sommer and Bäckhed, 2013; Douglas, 2018). The dynamic interaction between a microbiota and its host is under intense

53 scrutiny especially for mammalian species and a handful of model organisms (Colston and
54 Jackson, 2016; Douglas, 2019). However, very little is currently known on the biotic and abiotic
55 interactions between the microbiota of even well-known and classic vertebrate model
56 organisms such as amphibians (Colston and Jackson, 2016; Douglas, 2019; Rebollar and Harris,
57 2019).

58 The current paucity of knowledge on amphibian's microbiome is an historical thumb of
59 nose. Indeed in 1901, Olga Metchnikoff published a note on the influence of microbes on the
60 development of tadpoles (Metchnikoff, 1901). She concluded that microbes were vital to
61 tadpoles because they could not complete their development in sterile conditions, and her
62 results were confirmed by Moro (Moro, 1905). A few years later, these results were challenged
63 by Eugène Wollmann and his wife, who finally observed that *Rana temporaria* tadpoles could
64 complete their metamorphosis in sterile conditions (Wollman, 1913). They also reported that
65 tadpoles could be fed solely with bacteria, pinpointing their nutritive roles (Wollman and
66 Wollman, 1915).

67 Currently, the best-known amphibian model is the African clawed frog and it present
68 several features to unravel the interactions between an animal host and communities or
69 individual microbial taxa. *Xenopus* have a long lifespan of more than ten years and several tools
70 are available to study their biology including genomic engineering (Vouillot *et al*., 2014).
71 However, there is few data on *Xenopus* microbiota. Mashoof et al. used 16S rRNA
72 metabarcoding to describe the bacterial diversity in the gut microbiota of adult *Xenopus* and
73 found that *Firmicutes*, *Bacteroidetes* and *Proteobacteria* were the dominant bacterial phylum
74 like in the mammalian gut microbiota of human and mice (Mashoof *et al*., 2013).

75 Like many amphibians, *Xenopus* life history is characterized by an aquatic external
76 development. The embryo hatches after one or two days of embryonic development under the
77 protection of the chorion and of a double-layer jelly coat (Bles, E.J., 1906; Faber and

78 Nieuwkoop, 1994). The newly hatched embryo is in direct contact with its environment and it
79 usually sticks to the remnants of its jelly coat thanks to secretions from its adhesive gland. The
80 mouth will open one day later, and after about two more days, the small tadpole will start
81 feeding by filtering the water. Further growth and development occur during four weeks, a
82 period called premetamorphosis. This phase will be followed by prometamorphosis during
83 which significant growth of the limbs will occur. Finally the metamorphic climax during which
84 tail will resorb will end the morphogenesis and the adult-shaped froglet is completely formed
85 (Faber and Nieuwkoop, 1994; Brown and Cai, 2007). Most organs, including the gut, are found
86 in both tadpoles and adults but they experience a complete remodeling that enables the
87 continuation of their physiological functions in a different ecological niche (Hourdry *et al*.,
88 1996; Heimeier *et al*., 2010). Amphibian tadpoles are almost invariably water-dwelling
89 organisms, and most are microphagous with microbial fermentation contributing up to 20 % of
90 their energy uptake (Clayton, 2005; Pryor and Bjorndal, 2005; Altig *et al*., 2007). After
91 metamorphosis, froglets (imago) are still microphagous and as they grow they will prey on
92 larger animals, with a diet composed predominantly of chitin-rich insects and other arthropods.
93 The precise timing of organ and behavioral modifications depends on ecological traits and is
94 known in only a handful of species, including *Xenopus*. But as a *Pipidae*, *Xenopus* tadpoles,
95 metamorphs, froglets and adult frogs live predominantly in water (Bles, E.J., 1906).
96 Immunologically, post-embryonic development is hallmarked by significant changes
97 especially regarding mucosal immunity (Robert and Ohta, 2009; Pasquier, 2014; Colombo *et*
98 *al*., 2015). The climax of metamorphosis is hallmarked by high-levels of glucocorticoids that
99 cause a systemic immuno-depression (Rollins-Smith *et al*., 1997; Sachs and Buchholz, 2019).
100 Thus, amphibian metamorphosis is a post-embryonic developmental step during which host-
101 microbial interactions can play critical roles.

102 Changes in gut bacterial communities during anuran metamorphosis was first studied using
103 culturing methods and more recently using 16S rDNA gene metabarcoding (Fedewa, 2006;
104 Kohl *et al*., 2013; Vences *et al*., 2016; Chai *et al*., 2018; Warne *et al*., 2019; Long *et al*., 2020;
105 Zhang *et al*., 2020). A single study expanded its analysis using metagenomic and
106 metatranscriptomic (Zhang *et al*., 2020). These studies reported changes in the composition of
107 microbial communities upon metamorphosis, with differences between species.
108 We undertook this study to provide a description of the phylogenetic and metabolic profiles
109 of the gut microbiota from *Xenopus* tadpoles. We monitored the gut microbiome changes during
110 development and metamorphosis using 16S rDNA gene metabarcoding, metagenomic and
111 metatranscriptomic. We investigated the effect of the diet on tadpole's gut bacterial
112 communities. We identified the communities found in different adult organs, including the skin,
113 stomach, intestine and rectum. We also investigated the transmission of bacterial communities
114 between parents and their eggs.
115

116 # Results

117 ## Enumeration of bacterial cells in *Xenopus* tadpole's gut during development

118 We started to assess changes in tadpole's gut communities throughout development by
119 enumerating bacteria using flow cytometry (Figure 1). We selected six developmental stages
120 including young tadpoles that just started to feed, grown up tadpoles undergoing metamorphosis
121 up to adulthood (Figure 1A and Supplementary Figure 1). When we analyzed the distribution
122 of bacterial populations by relative size (forward scatter) and nucleic acid fluorescence, we
123 found that the samples from young tadpoles differed markedly from those of mature tadpoles
124 in their cytometric profiles (Figure 1A). While we observed a single cluster of bacteria in young
125 tadpole's guts, at least three such clusters could be distinguished in mature tadpoles. We also

126 observed that samples from tadpoles at the metamorphosis climax, from froglets and from adult
127 frogs gave the same distribution as the mature tadpoles (Supplementary Figure 1).

128 We determined an average of $1x10^6$ bacteria per individual at the young tadpole stage, $2x10^8$
129 at the prometamorphic stage and $3x10^7$ in the froglets (Figure 1B), indicating that the gut
130 bacterial mass increased just after the beginning of feeding and decreased simultaneously with
131 the gut size reduction observed during metamorphosis (Schreiber *et al*., 2005). We found that
132 the bacterial load changed significantly during development (ANOVA P-value = 0.041). The
133 difference between pre-feeding and premetamorphic tadpoles was significant (Tukey adjusted
134 P-value = 0.046). We also observed a tendency for difference between premetamorphic
135 tadpoles and Adults (Tukey adjusted P-value = 0.073); and between premetamorphic tadpoles
136 and froglets (Tukey adjusted P-value = 0.060).

137 Our data allow us to conclude that the tadpole's gut is colonized by a large population of
138 bacteria at the beginning of feeding, and that this bacterial population increases during tadpole's
139 development, then reduces upon metamorphosis before increasing again upon froglet growth.

140 *Xenopus* gut microbial diversity during development and metamorphosis

141 Since an important bacterial population was present in the tadpole's guts, we quantified the
142 taxonomic diversity of this microbiota. We set out mating experiments in which we sampled
143 whole tadpole's guts at different points of development up to adulthood and quantified bacterial
144 taxonomic diversity using 16S rRNA gene profiling. We compared 16s rRNA gene profiles
145 amplified from tadpoles at the premetamorphic stages of development (tadpoles, NF54 to
146 NF56), at the prometamorphic stages (prometamorphs, NF58 to NF61), at metamorphic stages
147 (metamorphs, NF 62), at the end of metamorphosis (froglet, NF66) and from sexually mature
148 adults. After filtering low abundance and singleton sequence clusters, we obtained an
149 abundance table for a set of 666 OTUs. According to a rarefaction curve analysis, our depth of

150 sequencing was sufficient to obtain a good sampling of the bacterial diversity in our sample set
151 (Supplementary Figure 2).
152 We examined which bacterial phyla accounted for these gut communities (Figure 2A and
153 Supplementary Figure 3). At the premetamorphic stage of development, we observed that
154 *Actinobacteria* dominated the tadpole's gut microbiota with an estimated abundance of 66.29%.
155 At this stage, *Proteobacteria* (mostly *Alphaproteobacteria*) and *Firmicutes* were also abundant
156 (17.65 and 13.20 %, respectively) while *Bacteroidetes* and *Verrucomicrobia* contributions were
157 quantitatively modest (1.58 and 1.28%, respectively). The tadpole's gut microbiota
158 composition changed with *Proteobacteria* becoming the major Phylum (63.33%, mostly
159 *Deltaproteobacteria*) in prometamorphic tadpoles, followed by *Firmicutes* (18.45%),
160 *Actinobacteria* (13.51%), *Bacteroidetes* (3.11%), *Synergistetes* (1.07%) and *Verrucomicrobia*
161 (0.53%). In metamorphic tadpoles *Proteobacteria* were more dominant (93.92%, mostly
162 *Alphaproteobacteria*), Firmicutes abundance decreased (5.15%) and *Bacteroidetes* (0.61%),
163 *Actinobacteria* (0.27%), *Synergistetes* (0.04%) and *Verrucomicrobiae* (0.01%) were minor
164 contributors. Once metamorphosis was completed, the gut microbiome of the froglets changed
165 and *Firmicutes* became dominant (62.56%), followed by *Proteobacteria* (32.49%, mostly
166 *Deltaproteobacteria*), *Bacteroidetes* (4.54%), *Actinobacteria* (0.39%), *Synergistetes* (0.01%)
167 and *Verrucomicrobia* (0.01%). In comparison, the composition of the adult gut microbiome
168 was marked by more balanced abundances of *Proteobacteria* (39.19%, mostly
169 *Deltaproteobacteria*) and *Firmicutes* (32.35%), a remarkable abundance of *Verrucomicrobia*
170 (13.30%) slightly higher than that of *Bacteroidetes* (11.94%), and a minor contribution of
171 *Synergistetes* (2.22%) and *Actinobacteria* (1.00%). The abundance patterns for *Proteobacteria*
172 were marked by different contributions of *Alpha* and *Deltaproteobacteria*. These patterns of
173 abundances at the phylum level were attributable to a restricted number of families
174 (Supplementary Figure 3A). At the family level, three genera from three families of

175 *Bacteroidetes* were predominant: *Bacteroides* (*Bacteroidaceae*) with a marked abundance
176 increase at froglet and adult stage, and dgA-11 (*Rikenellaceae*) with an increase during tadpole
177 growth and then in adult stages, and *Parabacteroides* (*Porphyromonadaceae*) that increased
178 only at the adult stage. *Verrucomicrobiaceae* was the dominant family of *Verrucomicrobia* in
179 adult guts, and it was represented by a single genus, *Akkermansia*. Similarly, a single unknown
180 genus of the *Synergistaceae* family was found at low abundance in *prometamorphic* tadpoles
181 and in Adults. *Synergistetes Microbacteriaceae* was the dominant family of *Actinobacteria* in
182 pre and prometamorphosis tadpole's guts, and it was represented by a single genus, *Leifsonia*.
183 Seven families of *Firmicutes* were predominant: *Lachnospiraceae* (several genera) and
184 *Peptostreptococcaceae* (one unknown genus) with a marked abundance increase at froglet and
185 adult stage; *Planococcaceae* (one unknown genus) that increased only at the adult stage;
186 *Clostridiaceae 1* (genus "*Clostridium sensu stricto 1*"), *Erysipelotrichaceae* (two genera
187 *Coprobacillus* and *Erysipelatoclostridium*) and *Ruminococcaceae* (genera
188 *Hydrogenoanaerobacterium*, *Anaerotruncus*, *Ruminococcaceae*) were found with fluctuating
189 abundances across the life stages, and finally Family XIII was found only at low abundance.
190 Eight families of *Proteobacteria* were predominant: *Aeromonadaceae* (genus *Aeromonas*),
191 *Neisseriaceae* (genus *Vogesella*) and a family of *Rhizobiales* (one unknown genus) dominated
192 the froglet gut microbiome; *Rhodospirillaceae* (one unknown genus) exhibited a tendency to
193 decrease across development and were minor in adults; *Desulfovibrionaceae* (genus
194 *Desulfovibrio*) were a minority at premetamorphosis and were abundant in the other stages,
195 *Pseudomonadaceae* (genus *Pseudomonas*) and *Bradyrhizobiaceae* (unknown genus) were
196 found in metamorph's guts, and *Rhodocyclaceae* (genus *Azovibrio*) in prometamorphic
197 tadpoles.

198 Altogether, we observed changes in the composition of the five most abundant bacterial
199 phyla making the gut microbiome as development proceeds, both during tadpole growth and

200 metamorphosis. The major shift during tadpole growth was a reduction of *Actinobacteria* and
201 an increase of *Proteobacteria*, and the transition to the adult lifestyle was marked by the
202 increase of *Synergistetes*, *Verrucomicrobia* and *Firmicutes*. This corresponded to a graded
203 increase of gram-negative bacteria during tadpole growth and development culminating at
204 metamorphosis before reducing thereafter (Supplementary Figure 3).

205 We also analyzed changes of OTU richness and phylogenetic diversity during development
206 (alpha diversity, Figure 2B, Supplementary Table 1 statistics). We identified two important and
207 significant changes: the first was an increase of bacterial species number and diversity that
208 occurred during tadpole growth between pre and prometamorphosis; and the second was the
209 opposite, namely a significant drop in species richness and diversity that occurred at the climax
210 of metamorphosis (Figure 2B and Supp. Table statistics). When focusing on a tadpole-adult
211 comparison, we found that the adult *Xenopus* gut microbiome contained about twice more
212 OTUs than the tadpole ones, and its phylogenetic diversity was 1.8 times higher. These
213 differences in microbiome diversity between the premetamorphic tadpole's guts and the adult
214 ones were significant using various alpha diversity metrics (Supplementary Table statistics).

215 In parallel to these changes of communities all across development, numerous OTU's were
216 shared between life stages. We found 111 OTUs (17%) present at all stages, that represented
217 22% of the adult gut microbiome and 29 to 38% of the other life stage microbiomes
218 (Supplementary Figure 4). Another set of 128 OTUs was shared between four life stages, 122
219 OTU's were shared between three, 151 between two and only 154 OTUs (23%) were found in
220 only one of the developmental stages (Supplementary Figure 4). The most prevalent OTUs were
221 detected with a threshold of very low relative abundances (< 5e-05 %, Supplementary Figure
222 4B). We found a set of ten OTUs that were both common and abundant; including an *alpha*
223 *proteobacterium*, three *Desulfovibrio*, a *Microbacterioaceae*, a *Clostridium stricto sensu*, two
224 *Hydrogenoanaerobacteria*, a *Rhizobiales* and a *Lachnospiraceae*. The abundances of the

225 *Alphaproteobacteria*, one *Desulfovibrio*, the *Clostridium sensu stricto* and the
226 *Lachnospiraceae* were the most homogeneous.

227 We searched more specifically which OTUs were characterized by a significant change of
228 abundance across developmental stages and identified a set of 22 OTUs corresponding to five
229 Phyla and 13 known genera (Supplementary Figure 5). The five OTUs most abundant in
230 premetamorph tadpole's gut but not in adult's gut were a *Microbacteriaceae* (*Actinobacteria*),
231 a *Rummeliibacillus* and a *Clostridium sensu stricto* 13 (*Firmicutes*), a *Bacteroides*
232 (*Bacteroidetes*) and an *Alpha-proteobacteria* (*Proteobacteria*). The opposite pattern, i.e. more
233 abundant in adult's guts, was hallmarked by a *Lachnospiracae* (*Firmicutes*), a *Synergistaceae*
234 (*Synergistetes*), a *Ruminococcaceae UCG-014* (*Firmicutes*), a *Rhizobiales* (*Proteobacteria*)
235 and an *Anaerorhabdus furcosa* group (*Firmicutes*).

236 Significant differences in community composition (beta diversity) were evidenced by
237 microbial community phylogenetic structure and ordination analysis (Figure 2C, Table
238 Statistics). The mean bacterial community structure and their dispersion differed according to
239 life stages (Supplementary Figure 6). The phylogenetic relatedness of communities changed
240 significantly during development, with negative and lower mean phylogenetic diversity values
241 found in metamorph and froglet samples indicating more phylogenetically clustered microbial
242 communities during metamorphosis. Overall, we conclude that the *Xenopus* gut bacterial
243 community succession during development and metamorphosis was associated with significant
244 dynamic changes of composition and structure.

245 *Xenopus* microbiota across several gut compartments

246 We then compared the bacterial diversity along the gut of adult frogs, thus we dissected the
247 gut in three parts: stomach, intestine and rectum. In parallel, we analyzed the bacterial
248 composition of the feces and the skin of these animals using 16S rRNA gene profiling. Whereas
249 *Bacteroidetes*, *Firmicutes* and *Proteobacteria* were the most abundant bacteria in the intestines,

250 the rectum, the feces and the skin microbiota, we observed that the *Tenericutes* (mostly
251 *Mollicutes*) were the most abundant in the stomach (Figure 3A, Supplementary Table statistics).
252 Surprisingly we observed a large quantity of *Acidobacteria* (28.8%) in only one feces sample.
253 The stomach, intestine and rectum microbiomes were well differentiated from each other in
254 composition and in structure analysis (PERMANOVA on bray-curtis dissimilarity F=6.93;
255 R2=0.43; p<0.001, Figure 3B and Supplementary Table statistics). Feces and skin microbiomes
256 were clearly separated from the other samples, but not between them.

257 Despite these differences, we identified 31 OTUs shared between the three gut sections: 16
258 were identified as *Bacteroidetes* (including 15 *Bacteroidia*), seven as *Firmicutes* (including six
259 *Clostridia*), six as Proteobacteria (including five *Desulfovibrio*), one *Parcubacteria* and one
260 *Synergistetes*. In conclusion, we showed that the bacterial diversity increased along the
261 anteroposterior axis of the adult *Xenopus* gut, from the stomach to the rectum, and the bacterial
262 community compositions and structures associated with those gut sections were also
263 significantly different (Supplementary Table statistics).

264 **Activity of the *Xenopus* tadpole gut microbiome at the onset of feeding**

265 We then wanted to know more precisely when bacterial communities started to be active
266 during development and what bacteria were found at the earlies stages of larval development.
267 When *Xenopus* embryo hatch, their mouth is not formed, the post-anal gut is open and the
268 archenteron is well formed. Feeding behavior will only start once mouth is formed and gut
269 organogenesis is more advanced, a few days later (Chalmers and Slack, 1998). We took
270 advantage of this situation to perform a first investigation of the succession of active bacterial
271 communities at early stages of larval development just after hatching when the mouth is not
272 open (NF 30), before (NF41) and after feeding (NF48); and in growing premetamorphic
273 tadpoles (NF50 and NF52). We set out experiments in which we followed-up embryos and
274 tadpoles from two egg clutches up to the completion of metamorphosis. We monitored

275 microbiome composition from pools of whole embryos or tadpoles starting at 24h after
276 fertilization using 16S rRNA sequencing on whole RNA extracts.

277 We observed an increase of bacterial species number and diversity up to feeding stage,
278 followed by a transient reduction at stage 50 (Supplementary Figure 7A). We found 103 OTUs
279 present across all stages, among which 11 were abundant OTUs (> 1%). At the earliest stage,
280 we observed that most bacterial activity was attributed to *Proteobacteria* (five OTUs:
281 *Rhodospirillaceae*, *Aeromonas*, *Rheinheimera*, *Pseudomonas*, *Desulfovibrio*) and
282 *Bacteroidetes* (two *Bacteroides* OTUs, one *Flectobacillus*, one *Rikenella*), that *Firmicutes*
283 (*Clostridium sensu stricto*) and *Synergistetes* (*Synergistaceae*) were already present while
284 *Fusobacteria* (*Fusobacteriales*) and *Verrucomicrobia* (*Akkermansia*) were minor contributors
285 (Supplementary Figure 7). We observed a different dynamic of bacterial community
286 successions between the two clutches. In one experiment, there was a gradual decrease of
287 *Proteobacteria* between NF30 and NF50, and an increase thereafter at stage NF52. This was
288 the converse for *Bacteroidetes*. In the other experiment, *Proteobacteriae* and *Synergistetes*
289 abundances oscillated with a decrease before and after feeding while the abundance of
290 *Bacteroidetes* oscillated in an opposite manner. This behavior was concomitant with a highest
291 abundance of *Synergistetes* that increased after feeding. In both clutches, *Firmicutes* proportion
292 increased up to feeding stage and decreased afterward. Altogether our results highlighted the
293 presence of a rapidly developing microbiota along the first stages of tadpole development,
294 characterized by a shift of the *Proteobacteria*/*Bacteroidetes* ratio.

295 We used the same strategy to monitor active bacterial communities in tadpoles at different
296 stages of metamorphosis using 16S rRNA sequencing on whole digestive tract RNA extracts.
297 We analyzed the prevalence and the abundance of bacteria as development proceeded. We
298 found a common set of 33 OTUs present in at least 50 % of the samples with a relative
299 abundance of 0.001% or more (Figure 4). All these OTUs were also found at early stages before

300 feeding, and in the gut of tadpoles up to the completion of metamorphosis (Figure 4B). The five
301 commonest OTUs were also the most abundant (> 0.01% abundance), and included unknown
302 or ill-defined species: a *Rikenella*, an *Alphaproteobacteria*, a *Bacteroides*, a *Desulfovibrio* and
303 a *Synergistaceae*. We found a few prevalent bacteria detected with low abundances such as an
304 *Alphaproteobacteria*, two *Ruminococcaceae*, a *Rikenella* and an *Haliscomenobacter*.

305 In a complementary analysis, we estimated the proportion of OTUs populating the adult gut
306 that originated from previous stages of development (Supplementary Figure 7). In both
307 experiments, the source of most OTUs was identified as the feeding tadpole's gut (52 and 95%),
308 a minority was identified as stemming from the embryos (3 and 19%). Altogether, we identified
309 that only few active bacteria found in the embryos before the feeding-stage will be later
310 populating the adult gut, and that a majority of tadpole's active bacteria will pass through
311 metamorphosis and be also present in the adult gut.

312 **Diet shapes *Xenopus* tadpole gut communities**

313 Since *Xenopus* tadpoles are suspension feeders, we hypothesized that tadpole's diets could
314 have an important impact on their active gut bacterial communities (Bles, E.J., 1906). We made
315 an experiment in which we fed tadpoles with a commonly used micro planktonic-based diet
316 (food 1) or a custom meal (food 2), and monitored their gut microbiome composition using 16S
317 rRNA sequencing on RNAs. Zoo and phytoplankton were used as ingredients for food 1 that
318 contained a higher level of fibers (6.4%) than food 2 (2.6%), and food 2 was sterile, devoid of
319 chitin and richer in available glucids 23.9%). The food regime did not change significantly
320 tadpole growth (Kruskal-Wallis chi-squared = 0.99, df = 1, p = 0.32) or development (Kruskal-
321 Wallis chi-squared = 0.34, df = 1, p = 0.56, Supplementary Figure 8). We found a total of 485
322 OTUs shared between the tadpoles fed with one or another diet, and this was making up the
323 majority of the OTUs found in each condition: 485 out of 581, i.e. 83% for food 1 and 485 out
324 of 531 i.e. 91% for food 2. We did not observe significant changes of OTU richness

325 ($\log_e$(W)=3.14, p=0.13) and phylodiversity using Faith's index, ($\log_e$(W)=3.33, p=0.29). The
326 differences of alpha-diversity measured using the Shannon or the Simpson indices were
327 significant ($\log_e$(W)=4.34, p=0.001 and $\log_e$(W)=4.30, p=0.004, respectively) pointing toward
328 a higher specific richness in tadpoles fed with food 1 (micro planktonic-based diet). This
329 difference was confirmed by comparing community structures: mean SES MPD was
330 significantly different ($\log_e$(W)=0.69, p=0.001), as did beta-diversity spread (global
331 PERMDISP F=13.42, df=1, N.perm=999, p=0.001). However, the mean SES MNTD was not
332 significantly different ($\log_e$(W)=3.93, p=0.377). The gut bacterial community from tadpoles fed
333 on food 2 (custom meal) was globally more phylogenetically even (Supplementary Figure 8).
334 The custom meal was associated with more *Synergistetes* at the expense of *Firmicutes* and
335 *Bacteroidetes* (Figure 5). The taxonomic and phylogenetic composition of gut bacterial
336 communities were also significantly impacted by the diet (PERMANOVA on bray-curtis
337 dissimilarity F=12.64, R2=0.44, p=0.001 and on MNTD dissimilarity F=29.13, R2=0.64,
338 p=0.001), as evidenced on an ordination plot (Figure 5). The relative abundances of all five
339 most abundant Phylum differed according to the diet, the most notable being the *Synergistetes*
340 that accounted for 0.05 to 0.76% in the planktonic diet condition and for 0.80 to 17.72% in the
341 sterile diet condition (Figure 5). We found 82 OTUs whose abundance differed significantly
342 according to diet (Supplementary Figure 6). For example, *Chitinophagacae* were abundant in
343 the tadpoles fed with the micro planktonic-based diet, while a *Sphingobacteriales* was most
344 abundant in tadpoles fed with the artificial diet. Altogether, we observed that *Xenopus* tadpoles
345 gut microbial communities could be shaped by their diet without a noticeable impact on growth
346 and development.

347 ## *X. tropicalis* microbiome transmission

348 Knowing the transmission mode of bacterial communities across individuals and generations is
349 a recurrent question in the study of animal microbiomes. We set out an experiment to evaluate

350 the inheritance of bacterial communities between *Xenopus* parents and their clutch of eggs. We
351 performed eight independent crosses and sampled the skin and the feces of both parents along
352 with their egg clutch. When we looked at bacterial phylum diversity, we found that feces
353 contained more *Verrucomicrobia* and *Firmicutes*, while both skin and eggs contained more
354 *Proteobacteria* (Figure 6). In one case, we observed a resemblance between eggs and the feces
355 of one parent. Globally, the bacterial communities of the skin and of the eggs were significantly
356 more similar to each other than those from feces in terms of community structure and
357 composition as evidenced using different metrics (Figure 6, Supp. Table statistics). We also
358 analysed the proportion of the egg bacteria derived from adult skin and feces. In five out of the
359 eight crosses, more than 70% of the bacteria found in the eggs were not from feces or the skin
360 of the parents. In the three other crosses, we observed that male or female skin made up to 75%
361 of the egg bacteria. In conclusion, we found that the main drivers of egg bacterial communities
362 were the environment and the skin of the parents, with the feces being only minor contributors.

363 Whole shotgun metagenomic and metatranscriptomic analysis of *X. tropicalis* 364 gut microbiota

365 In the final part of our study and since few studies have investigated the genomic functions
366 of the amphibian microbiome, we used a whole shotgun metagenomic and metatranscriptomic
367 approach to better characterize the *Xenopus* gut microbiota and its activity in the guts of
368 prometamorphic tadpoles (Figure 7). Globally, both methods gave the same taxonomic profiles
369 and were concordant with the 16S rRNA gene metabarcoding approach while giving a finer
370 taxonomic resolution. We observed four main dominant phyla: *Bacteroidetes* (mostly
371 *Bacteroides*), *Proteobacteria* (mostly *Desulfovibrio* and *Polynucleobacter*), *Firmicutes* (mostly
372 *Ruminococcus*) and *Actinobacteria* (mostly *Microbacterium*) (Figure 7A). *Bacteroidetes* were
373 the most dominant phylum representing 46.5% of the population using a metagenomic survey
374 and 49.3% using the metatranscriptomic survey. *Proteobacteria* represented 16.6% and 20.9%,

375 while *Firmicutes* represented 7.1% and 11.4% of the bacterial population in the metagenomic
376 and metatranscriptomic data, respectively. *Actinobacteria* relative abundance was 17.4% in
377 metagenomic survey but represented only 4.4% in the metatranscriptomic data.
378 *Verrucomicrobia* represented 5.5% of the sequences in the metatranscriptomic data but it was
379 less observed in metagenomic data with only 1.1% of the bacterial content.

380 When we sorted out the 15 most abundant species, defined as being those representing more
381 than one percent of the bacterial content each, we found that nine of them were also common
382 in the mammalian gut microbiota (Figure 7B). A main dominant species observed in the
383 tadpole's gut was *Bacteroidetes fragilis*, a common bacterium found in mammalian's gut
384 microbiota. *Bacteroidetes thetaiotaomicron,* known to be the main dominant species in the
385 human gut microbiota, represented more than four percent of tadpole's gut microbiota. The
386 presence of another species, *Polynucleobacter necessarius* was interesting because it can be
387 found either free or as an endosymbiont of eukaryotic ciliates (Boscaro *et al*., 2013). Among
388 those 15 bacteria, 11 are strictly anaerobic, two are facultative anaerobic and two are aerobic.

389 In conclusion, we confirmed that the *X. tropicalis* tadpole's gut microbiota harbors a large
390 amount and diversity of bacterial cells, mainly constituted of anaerobic bacteria and common
391 bacteria at the species level with mammalian gut microbiota.

392 *Xenopus tropicalis* gut microbiota genes catalog

393 To characterize the *Xenopus* microbiome, we compiled a gene catalog from our
394 metagenome and metatranscriptome data sets. We assembled the metagenome reads in 51,060
395 scaffolds. Although the median size of the scaffolds was 817 bp, 25 scaffolds were significantly
396 longer and reached more than 100,000 bp including two scaffolds longer than 200,000 bp.
397 These long scaffolds probably corresponded to abundant bacteria in the *Xenopus* tadpole's gut
398 microbiota.

399 We analyzed the GC percent composition and the number of reads mapped at each position
400 along these long scaffolds to check the quality of their assembly. The GC percent remained
401 relatively constant all along the scaffold (Supplementary Figure 7) and the numbers of reads
402 mapped all along the scaffolds were significant, with at least 10 reads for each position
403 (Supplementary Figure 8). Therefore, each of these scaffolds seems to be derived from a
404 different genome.

405 We performed a gene prediction analysis on each scaffold and predicted 82,679 CDS. A
406 subset of 32,584 CDS (39.4%) was also associated with 6,713 unique UniProtKB identifiers.
407 These predicted CDS correspond to the first gene catalog of a *Xenopus* tadpole's gut microbiota.
408 To better characterize this microbiota, we investigated the level of expression of each CDS by
409 mapping metatranscriptomic reads on these CDS. At least one metatranscriptomic read could
410 be mapped on 23,349 CDS out of the 82,679 predicted CDS (28.2%). We refer to these CDS
411 as expressed CDS (eCDS). For more than 95.0% of these eCDS, the relative expression level
412 was between 0 and 100 RPK while some eCDS were highly expressed with a relative expression
413 higher than 10 000 RPK.

414 Among those eCDS, 7,071 (30.3%) were classified as hypothetical proteins, they were
415 observed in both low and highly expressed eCDS. For example, the eCDS with the highest
416 relative expression, 41 122 RPK, was identified as a hypothetical protein but we couldn't find
417 any homolog sequence using nucleic or amino acid comparison with BLASTn and BLASTp
418 against the NCBI nucleic and protein NR database, the NCBI protein env_nr database, or even
419 the nucleic and protein from the human gut microbiome gene catalog.

420 Then, we compared the *Xenopus* and the human gut metagenomes. When both
421 metagenomes were compared by functional annotation, we found that 2,243 (88.2%) out of the
422 2,542 unique KEGG Orthology (KO) identifiers associated with the *Xenopus* gut metagenome
423 genes were also observed in the KO identifiers of the human gut metagenome. However, the

424 similarities between both metagenomes were less important in terms of nucleic and amino acid
425 sequences. Only 2,372 (2.9%) and 4,603 (5.6%) of the *Xenopus* CDS were in common with the
426 human microbiome, using BLASTn and BLASTp comparisons filtered for 95.0% of identity
427 and 90.0% of coverage.

428 In conclusion, we identified 82,679 CDS from the *X. tropicalis* tadpole gut metagenome.
429 Using metatranscriptomic sequencing, we revealed that about 28.2% of these protein sequences
430 are highly transcribed. About 59.8% of these protein sequences are not well annotated,
431 whatever their expression level inferred from metatranscriptomic. A 40.2% fraction of well-
432 known proteins encode at least 6,713 non-redundant protein functions. Our data also show that
433 a majority of these known protein functions are shared with the human gut metagenome, and
434 could be identified as a 'core functional tetrapod metagenome'.

435 Metabolic profile of the *Xenopus* gut microbiota

436 To better characterize the metabolic capacity of the *Xenopus* tadpole's gut microbiota, we
437 used the eggNOG annotation to analyze the distribution and the relative expression of metabolic
438 pathways in the predicted CDS that had an UniProtKB identifier (Figure 8) (Powell *et al.*,
439 2014). Most of those CDS (42.5%) were assigned to the "metabolism" annotation class of
440 eggNOG, and they were also the most expressed ones (35.8%). Most of the 'metabolism'
441 expression dealt with the energy production (11.5%), amino acid metabolism (6.9%) and
442 inorganic ion metabolism (6.5%). A part of the CDS (24.9%) was assigned to the "cellular
443 processes and signaling" category. The most expressed sub-category was the 'posttranslational
444 modification, protein turn over and chaperones' (13.1%), the other main expressed category
445 focus on the cell structure, communication and motility (4.5%, 3.9% and 5.1%). Another part
446 of the CDS (21.5%) were assigned to the "information storage and processing" category. Not
447 surprisingly the most expressed category concerned the translation and the ribosomal structure
448 and biogenesis (19.6%), the transcription (6.3%) and the replication (3.4%).

449 Next, we compared the metabolic pathways encoded by the *X. tropicalis* gut metagenome
450 with those encoded by the *X. tropicalis* genome (Supplementary Figure 9). We found shared
451 pathways such as the synthesis of the neurotransmitter GABA by a glutamate decarboxylase
452 provided by both the *Xenopus* nuclear genome and its gut microbiome. As an example of
453 microbiome added pathway, we identified the known mammalian case of a tryptophanase
454 encoded by the gut metagenome that enables the synthesis of L-Formylkynurenine from L-
455 tryptophan. We identified 742 KO identifiers encoding the same function, mostly common and
456 central metabolic functions like the glycolysis pathway. However, a set of 2011 pathways were
457 uniquely provided by the gut metagenome, and were responsible of its metabolic specificity.

458 **Discussion**

459 We report that a large community of bacteria develop in the tadpole alimentary canal as soon
460 as feeding starts and it peaks before metamorphosis. While the gut microbiome biomass reduces
461 significantly at metamorphosis, it remains important. This probably reflects the feeding
462 behavior of *Xenopus* at metamorphosis: Naitoh and colleagues reported that filter feeding can
463 be observed in metamorphs up to stage NF59-NF61, and adult-like feeding starts at stage NF63
464 (Naitoh *et al.*, 1989). Thus, there is only a short period of time, two to three days, during which
465 the *Xenopus* metamorph stops feeding. Also, the gut itself starts to shorten at the metamorphic
466 stage NF62 and will reduce four-fold to its adult-like length by stage NF66 (Schreiber *et al.*,
467 2005; Heimeier *et al.*, 2010). This means that adult feeding behavior occurs before the
468 completion of gut remodeling, and that tadpole and adult digestive physiology overlap at the
469 end of metamorphosis. In an animal-house setting, we deem it likely that *Xenopus* froglets
470 continue to eat the available plankton in the rearing aquarium as long as a new diet is not
471 artificially imposed to them, because they rely upon suction feeding as adults (Bles, E.J., 1906).
472 More generally, the change of eaten food composition is likely to be gradual depending on the
473 ecology of the amphibian species considered. For example, Fedewa reported insect material in

474 the guts of *Bufo terrestris* and *Pseudacris crucifer* at Gosner stage 45-46 (NF64-NF65) i.e. in
475 metamorph before the completion of metamorphosis, and the interval of fasting was the
476 beginning of metamorphosis (Gosner stages 42-44, NF60-NF63) (Fedewa, 2006).

477 Our DNA and RNA 16S metabarcoding data further demonstrated that the colonization of
478 the tadpole by microorganisms occurred early during *Xenopus* tadpole development. Moreover,
479 our results proved that *Xenopus* gut bacterial communities change during tadpole development
480 and metamorphosis. At first, i.e. before and right after feeding, the change in composition of
481 the microbiota is characterized by an increase of the *Bacteroidetes* / *Proteobacteria* ratio. The
482 overall diversity of the microbiota seems to be reduced just before feeding, possibly because of
483 the development and the activity of innate immune responses of the newly hatched larvae
484 (Pasquier, 2014). After an increase of the microbiota diversity, once feeding started, there is
485 another step of reduction that we interpret as the result of an adaptation of the environmental
486 bacterial population to the tadpole's gut environment. In this period, when the tadpole starts
487 feeding and grows rapidly (NF45 to NF56), there are 1,000 times more bacteria but the
488 microbiota composition remains quite the same. During metamorphosis, we observed an
489 important diminution of the bacterial abundance within and a change of diversity. Indeed
490 metamorphosis is associated with several modifications of the gut organs and we expected that
491 gut reduction and neuroendocrine changes would impact the gut microbiota, as shown
492 previously for other species (Fedewa, 2006; Kohl *et al.*, 2013; Vences *et al.*, 2016; Chai *et al.*,
493 2018; Warne *et al.*, 2019; Long *et al.*, 2020; Zhang *et al.*, 2020).

494 The bacterial diversity observed in the *X. tropicalis* gut was consistent with the results of
495 Mashoof et al. on the diversity observed in *X. laevis* gut (Mashoof *et al.*, 2013). Indeed, the
496 same three phyla dominating the gut microbiota were observed in both analyses. The
497 dominance of *Firmicutes*, *Bacteroidetes* and *Proteobacteria* is also a characteristic of the
498 vertebrate gut in general (Colston and Jackson, 2016; Youngblut *et al.*, 2019). Moreover the

499 *Xenopus gut* microbiota diversity increased following the anteroposterior axis of the gut, as
500 observed in human gut microbiota (Sekirov *et al*., 2010).

501 We found that the abundance of several *Bacteroides*, *Bilophila* and *Lachnospiraceae*
502 bacteria increase during tadpole development and metamorphosis. These bacteria are well-
503 known to be abundant in the gastro-intestinal tracts of numerous vertebrates, including man,
504 and characterized by their resistance to high concentrations of bile salts or their bile acid
505 hydrolase activities (Song *et al*., 2019). We therefore propose an interpretation of our findings
506 in light of bile acids being key molecular components regulating the gut microbiome
507 composition during amphibian development and metamorphosis. Bile acids are small
508 molecules produced mainly in the liver from cholesterol and further metabolized in the gastro-
509 intestinal tract. They are known to act as molecular messengers between the host and their gut
510 microbiota: on the host side, they play a role in numerous metabolic pathways via their cellular
511 receptors and on the microbiome side they can modulate bacterial growth directly and indirectly
512 (Ridlon *et al*., 2014; Wahlström *et al*., 2016). Bile acids can act directly on the gut microbiome
513 because they have intrinsic antimicrobial activity and indirectly because their host cellular
514 receptors regulate antimicrobial peptides genes. In turn, some bacteria encode bile hydrolases
515 that enable the production of secondary bile acids (Joyce *et al*., 2014; Song *et al*., 2019).
516 Therefore, we can consider bile acid composition as a trait of strong evolutionary significance
517 since it links nutrition, gut, liver and gill physiology, host genome evolution and the gut
518 microbiome composition (Reschly *et al*., 2008; Hofmann *et al*., 2010; Ridlon *et al*., 2014). In
519 amphibians, bile acids are present in tadpoles but they increase in quantity and complexity after
520 metamorphosis (Anderson *et al*., 1979; Cole and Little, 1983; Reschly *et al*., 2008). It is known
521 that bile acids composition and complexity increase due to changes in host gene expression.
522 We hypothesize that ontogenetic and endocrine regulation of amphibians host genes such as
523 the bile acid nuclear receptor (Farnesoid X receptor, FXR; NR1H4), or its surface G-protein

524 coupled receptor (TGR5) could be initial regulators of gut microbiome composition. FXR, an
525 intra-cellular bile acid-sensing transcription factor of the nuclear factor superfamily, regulates
526 bile acid and lipid homeostasis, and other genes such as FOR in *Xenopus* may play similar roles
527 using different ligands (Seo *et al*., 2002; Reschly *et al*., 2008; Frisch and Alstrup, 2018). It is
528 noteworthy that in mice TGR5 has been shown to link bile acid and thyroid hormone signaling
529 by promoting intracellular thyroid hormone activity via the induction of deiodinase 2 in brown
530 adipose tissue (Watanabe *et al*., 2006). In future studies, manipulation of gene activities, of bile
531 acid composition and concentration and of the microbiome could be used to unravel the
532 diversity and the evolution of these regulations in amphibians and other vertebrates.

533 We provide evidence that the diet of *Xenopus* tadpoles affected the diversity of their gut
534 microbiome and thus that the mucosal immunity of tadpoles can interact with a variety of
535 bacterial communities (Figure 5). Tadpoles fed a micro planctonic-based diet had a gut
536 microbiome with a higher specific richness compared with tadpoles fed a sterile flour-diet. The
537 latter diet was associated with a lack of *Chitinophagacae* involved in chitin degradation. These
538 results contribute to the growing body of evidence that diet as an environmental factor can
539 affect the composition of the gut microbiota.

540 Maternal transmission of microbes in animals is a well-known phenomenon but its
541 documentation in amphibians is restricted to only few examples (Funkhouser and Bordenstein,
542 2013; Walke *et al*., 2014; Warne *et al*., 2019). In amphibians like in other animals, the
543 transmission of microbial communities can be horizontal, vertical or environmental. The
544 vertical transmission mode may depend critically on the reproduction behaviour of the animals.
545 In *Xenopus,* the natural mating behaviour of the couple in amplexus involves looping dances
546 from the bottom to the surface. Eggs are mostly laid by the female when she is near the surface,
547 and immediately fertilized by the male. These movements may lead eggs to stick to the skin of
548 either parent, and since the skin of amphibians harbours a rich microbiota, it can constitute a

549 vector of vertical transmission from either parent. In addition, the eggs are laid through the
550 female cloaca, and the sperm is also emitted by the male cloaca. Since the cloaca is a common
551 anatomical structure shared by the reproductive, excretory and digestive systems, the microbial
552 communities of these three systems may be transmitted to the eggs. Here we sampled the skin
553 and feces of both parents to quantify the transmission to the eggs. We found that quantitatively
554 and using the Bayesian algorithm of source tracker, the bacteria found on the eggs were mostly
555 coming from the environment, and the second source was the skin of either parent. It was
556 notable that a *Chitinimonas* species, a bacterium known to synthesize the antifungal Violacein,
557 was one of the OTU transmitted from both parents in all crosses. This is relevant with
558 *Saprolegnia* egg infections and with chytridiomycosis. Recently, Warne and collaborators
559 reported that changes of the woodfrog egg microbiota influenced the bacterial communities at
560 later larval stages (Warne *et al*., 2017, 2019).

561 *Bacteroidetes*, *Firmicutes* and *Proteobacteria* were slightly more represented in the
562 metatranscriptome than in metagenome highlighting that those bacteria were present and active
563 in the tadpole gut. Actinobacteria were less abundant in metatranscriptome than metagenome,
564 showing a reduced activity. On the contrary, we found that *Verrucomicrobia* were very active.

565 Our data showed a functional similarity between the metagenomes from *Xenopus* and
566 mammalian guts, with at least 88.2% of shared metagenome genes functions. Yet this similarity
567 was only observed in term of functional annotation and not for nucleic and amino acid
568 composition of the metagenomic genes. Thus, we can predict that these common functions are
569 encoded by relatively close bacterial species. These results are consistent with the previous
570 observations of Xiao et al. when they compared the catalogs of gut metagenome genes from
571 mice and human, and observed 92.5% of common functions but only 4.0% of common genes
572 (Xiao *et al*., 2015).

573 Our data highlighted the important capacity of the microbiota to complement the metabolic
574 pathways of the *Xenopus* genome. In terms of metabolic capacity, genes involved in 'energy
575 production and conversion' were the most expressed, emphasizing the importance of the energy
576 production by the microbiota within the interaction with its host. In the functional category
577 'cellular processes and signaling', genes involved in cell structure, motility and transduction
578 signal were the most expressed. This observation is consistent with the idea that the microbiota
579 forms an ecosystem with highly active bacteria interacting with each other and with the host.
580 The need to perform investigations on animals from natural populations has rightly been
581 underscored, for example by an interesting review of Sarah Hird (Hird, 2017). Yet we face
582 several methodological difficulties when it comes to sample natural populations. In some
583 studies, animals have been captured in the wild and raised thereafter in a laboratory setting. The
584 current global threats on amphibians makes such studies difficult to realize and restricts
585 severely the breadth of species that can be studied. In addition, the capture of vertebrate animals
586 induces a variable amount of stress, leading to different responses including an
587 immunosuppression (Rollins-Smith *et al*., 1997; Narayan, 2013). While the effect of captivity
588 on amphibian microbiomes has been documented, there is a considerable room for possible
589 explanations (Becker *et al*., 2014; Loudon *et al*., 2014; Bataille *et al*., 2016). Also, parasitism
590 is common in natural populations, and it can represent a hidden variable of considerable
591 importance in microbiome studies. For example, the mutualism between the nematode
592 *Gyrinicola batrachiensis* and *Rana catesbeiana* leading to a quicker tadpole development has
593 been linked to the hindgut fermentation capacity (Pryor and Bjorndal, 2005). Studies on
594 laboratory animals for which rearing conditions are more uniform, with the potential for a better
595 control of parameters and for reproducing experiments in different laboratories are definitively
596 needed to make the link with investigations on natural populations. In this regard, *Xenopus*
597 represents an interesting model since it is a widespread anuran with more than 20 species

598 described in sub-Saharan Africa, most species are classified of least-concern according to
599 IUCN, and there is a vast body of biological knowledge relating to its development, its
600 physiology and its genetic. We hope that our study will constitute a background knowledge
601 enabling future work in the study of amphibian-microbial symbioses.

602 Conclusions

603 In summary, we described the bacterial components of the *Xenopus* gut microbiota, the
604 adult gut biogeography, the succession of communities during ontogeny, the impact of the
605 alimentation in shaping the tadpole's gut bacterial communities, the transmission of skin and
606 fecal bacteria to the eggs. We also identified the most active gut bacteria and their metabolic
607 contribution to the tadpole physiology and showed the close resemblance between amphibian
608 and mammalian gut microbiome. Keeping in mind the advantages of the *Xenopus* model, our
609 data provided evidences that *X. tropicalis* raised in animal facilities is highly suitable for host-
610 microbiota studies. Our study contributes to the growing body of research on the study of
611 bacterial symbiosis in amphibians and on the evolutionary associations between amphibians
612 and their microbiota. Further studies on the dynamics of the *X. tropicalis* gut microbiota during
613 early development and metamorphosis should provide useful information on the evolution of
614 host-microbiota interactions in vertebrates.

615

616 Methods

617 Animals and animal husbandry

618 We used *Xenopus tropicalis* frogs from the TGA and Sierra Leone strains and we let them
619 reproduce using induced natural mating as described in the supplementary materials and
620 methods. Parents were transferred back to their housing tank while the embryos were let in the

621 mating tanks. Tadpoles were reared in static water throughout embryogenesis and
622 metamorphosis.

623 Tadpoles and adults were euthanized with tricaine methane sulfonate pH 7.5 at 5 $g.L^{-1}$. We
624 used the Nieuwkoop and Faber table of development to identify tadpole's developmental stages
625 (Faber and Nieuwkoop, 1994).

626 Bacterial purification from tadpole's intestinal tract

627 We dissected euthanized tadpoles in phosphate buffered saline (PBS) to collect the gastro-
628 intestinal from the stomach to the rectum. For the sake of simplicity, we used the term "gut" to
629 refer to the whole gastro-intestinal tract of tadpoles or adults throughout the manuscript. We
630 homogenized each intestinal tract in 500 µL of ice-cold PBS using a Potter-Elvehjem
631 homogenizer. We then prepared a concentrated bacteria extract by successive filtrations on 40,
632 20 and 5 µm filters (nylon 40 µm cell strainer from BIOLOGIX; 20 µm net ring from Pharmacia
633 Fine chemicals; Whatman® Puradisc 13 syringe filters 5 µm from SIGMA-ALDRICH®).
634 Next, we harvested the cells by centrifugation at 13 000g for 15 min at room temperature. These
635 pellets were then used for nucleic acid extraction as detailed in Supplementary materials and
636 methods, for fixation and microscopy or flow cytometry analysis (Figure 1).

637 Flow cytometry analysis

638 We prepared triplicate samples from tadpoles at stages NF45-48, NF51-54, NF56, NF60-
639 61, 15 days froglets and adults. Each sample was made from five tadpole's guts per replicate
640 for the NF45-48 and NF51-54 stages, single individuals were used for later developmental
641 stages. We fed the tadpoles two days before the first time point (stage NF45-48), and ten days
642 before sampling the froglets. We prepared the filtered bacterial cell samples as described
643 previously and we fixed the resuspended bacterial pellet in 1.0% paraformaldehyde at 4°C
644 during 2 h. We analyzed samples prepared by mixing fluorescent beads with bacteria stained
645 using propidium iodide with a MoFlo® Astrio™ cytometer (BECKMAN COULTER). Each

646 measure was done in triplicate to compute a mean value and the standard deviation for each
647 biological replicate sample.

648 **Metagenome and metatranscriptome sequencing**

649 We prepared genomic DNA (gDNA) and RNA from 5 µm filtered gut samples obtained
650 from five *X. tropicalis* tadpoles at stage NF56 raised in the same aquarium. Metagenomic and
651 metatranscriptomic sequencing were performed by the Beijing Genomics Institute (BGI) using
652 an Illumina® HighSeq™ 2500. The insert sizes of the metagenomic and metatranscriptomic
653 libraries were 170 bp and 180 bp, respectively. We obtained 23 639 893 and 20 000 000 high
654 quality 100bp paired end sequences for metagenomic (ERS716504) and metatranscriptomic
655 (ERS716505), respectively.

656 **16S rRNA and 16S rDNA library construction and sequencing**

657 gDNA or RNA were used as template for 16S Ribosomal RNA (16S rRNA) or DNA (16S
658 rDNA) amplification. A detailed list of samples used for the 16S rDNA and rRNA library
659 construction is given in supplementary table 1. A first PCR was performed to amplify the V3-
660 V4 variable region of the 16S rDNA and rRNA; the PCR condition details and
661 oligonucleotide sequences are given in Supplementary information. The PCR products were
662 sent to the GeT sequencing facility (France Génomique, INRA, Toulouse) for library
663 preparation and sequencing. PCR products were purified and quantified by spectrophotometry
664 and a second PCR was performed to integrate a barcode index. The barcoded PCR products
665 were pooled and their quality was checked using capillarity electrophoresis and quantitative
666 PCR. Finally, the PCR products were sequenced using a Miseq (supplied by Illumina®). We
667 obtained a total of 3,647,548 clean read counts from 132 samples. The metadata and number
668 of sequences obtained by sample is given in Supplementary Table 1.

669 **16S rRNA and 16s rDNA sequence analysis**

670 We sequenced 62 samples and obtained an average of 25,218 assembled paired-end
671 sequences per sample, with a minimum of 8,134 and a maximum of 66,578. We used the FROG
672 pipeline for OTUs identification and taxonomic affiliation (Escudie *et al*., July 6th to 9th).
673 Overlapping reads were assembled and sequences were dereplicated before clustering using the
674 SWARM algorithm. Chimeric sequences were then removed and OTUs were filtered on
675 abundance for at least 0.005%. Taxonomic affiliation of the OTUs was performed based on the
676 16S Sylva database (V.123) using blast and RDP classifier.
677 We used script implemented in R to perform different microbiome community analysis
678 (provided on GitHub at https://npollet.github.io/metatetard/) (R Core Team, 2019). Source-
679 sink analysis was performed using Feast (Shenhav *et al*., 2019).

680 Taxonomic assignment for metagenome and metatranscriptome sequences

681 We used the taxonomic assignment results provided by the BGI for the metagenomic
682 analysis. We performed taxonomic assignment from metatranscriptomic reads using
683 SortMeRNA (Kopylova *et al*., 2012) with default parameter to extract the reads derived from
684 16S rRNA and the Ribosomal Database Project (RDP) classifier to obtain the taxonomic
685 assignment (Wang *et al*., 2007).

686 Metagenome assembly and gene prediction

687 We used Ray Meta assembler v2.3.1 to assemble metagenome reads. We obtained 51,060
688 scaffolds, the scaffolds size varying from 500 bp to 296,477 bp with a median size of 817 bp
689 (Supplementary Materials and Methods). We analyzed the ten longest scaffolds by mapping
690 reads and computing GC percent composition as detailed in Supplementary Materials and
691 Methods and shown on Supplementary Figures 3 and 4.
692 We predicted 82 679 CDS on the assembled metagenome scaffolds using Prokka v.1.10
693 (Seemann, 2014). These predicted CDS were analyzed to identify their function, their relative

694 expression and were compared with the human gut microbiota gene catalog as indicated in
695 Supplementary Materials and Methods.

696 List of abbreviations

697 NF: Nieuwkoop and Faber developmental stage

698 Declarations

699 **Ethics approval and consent to participate**: We used standard rearing conditions for
700 *Xenopus* tadpoles and adults and all animal experiments were conducted in accordance with
701 the regulation on Animal Experimentation (registration number 91–401).

702 **Consent to publication:**

703 Not applicable

704 **Availability of data and material:** The sequence datasets generated and/or analyzed during
705 the current study are available in the EMBL Nucleotide Sequence Database (ENA),
706 metagenomic (ERS716504) and metatranscriptomic (ERS716505)
707 https://www.ebi.ac.uk/ena/data/view/PRJEB9311. 16S rRNA gene sequence data are available
708 at https://www.ebi.ac.uk/ena/data/view/PRJEB38248.

709 Other data type supporting the findings are available within the article and its supplementary
710 files.

711 **Competing interests:** The authors declare that they have no competing interests.
712

713 **Funding:**

714 We used the Data Intensive Academic Grid conducted on the National Science Foundation
715 funded MRI-R2 project #DBI-0959894" to perform some of the bioinformatic analyses. The
716 cytometry facilities of Imagerie-Gif (http://www.i2bc.paris-saclay.fr/spip.php?article279) is
717 member of the Infrastructures en Biologie Santé et Agronomie (IBiSA), and is supported by
718 the French National Research Agency under Investments for the Future programs "France-

BioImaging", and the Labex "Saclay Plant Science" (ANR-10-INSB-04-01 and ANR-11-IDEX-0003-02, respectively).

Author's contributions: All authors read and approved the final manuscript. TS and IC performed all experimental work under the guidance of NP. TC performed whole genome shotgun sequence analysis. NP performed 16S rRNA gene sequence analysis. TS and NP wrote the manuscript.

Acknowledgements

We are grateful to the Genotoul bioinformatics platform Toulouse Midi-Pyrenees (Bioinfo Genotoul) for providing computing and storage resources. The present work has benefitted from the facilities and expertise of the cytometry facilities of Imagerie-Gif, (http://www.i2bc.paris-saclay.fr/spip.php?article279). We thank Catherine Zanchetta and the team of the GeT facility for 16S metabarcoding sequencing. We thank Odile Bronchain, Albert Chesneau and Muriel Perron for providing access and use of their *Xenopus* animal facility in Orsay. We thank Jean-Michel Rossignol for critically reading our manuscript.

Conflict of Interest

None

References (100 max)

Altig, R., Whiles, M.R., and Taylor, C.L. (2007) What do tadpoles really eat? Assessing the trophic status of an understudied and imperiled group of consumers in freshwater habitats. *Freshw Biol* **52**: 386–395.

743 Anderson, I.G., Briggs, T., Haslewood, G.A., Oldham, R.S., Schären, H., and Tökés, L.
744 (1979) Comparison of the bile salts of frogs with those of their tadpoles. Bile-salt changes
745 during the metamorphosis of Rana Catesbeiana Shaw. *Biochem J* **183**: 507–511.
746 Bataille, A., Lee-Cruz, L., Tripathi, B., Kim, H., and Waldman, B. (2016) Microbiome
747 Variation Across Amphibian Skin Regions: Implications for Chytridiomycosis Mitigation
748 Efforts. *Microb Ecol* **71**: 221–232.
749 Becker, M.H., Richards-Zawacki, C.L., Gratwicke, B., and Belden, L.K. (2014) The effect of
750 captivity on the cutaneous bacterial community of the critically endangered Panamanian
751 golden frog (Atelopus zeteki). *Biol Conserv* **176**: 199–206.
752 Bles, E.J. (1906) The life history of Xenopus laevis, Daud. *Trans R Soc Edin* **41**: 789–821.
753 Bordenstein, S.R. and Theis, K.R. (2015) Host Biology in Light of the Microbiome: Ten
754 Principles of Holobionts and Hologenomes. *PLoS Biol* **13**: e1002226.
755 Boscaro, V., Felletti, M., Vannini, C., Ackerman, M.S., Chain, P.S.G., Malfatti, S., et al.
756 (2013) Polynucleobacter necessarius, a model for genome reduction in both free-living and
757 symbiotic bacteria. *Proc Natl Acad Sci U S A* **110**: 18590–18595.
758 Brown, D.D. and Cai, L. (2007) Amphibian metamorphosis. *Dev Biol* **306**: 20–33.
759 Chai, L., Dong, Z., Chen, A., and Wang, H. (2018) Changes in intestinal microbiota of Bufo
760 gargarizans and its association with body weight during metamorphosis. *Arch Microbiol* **200**:
761 1087–1099.
762 Chalmers, A.D. and Slack, J.M. (1998) Development of the gut in Xenopus laevis. *Dev Dyn*
763 *Off Publ Am Assoc Anat* **212**: 509–521.
764 Clayton, L.A. (2005) Amphibian gastroenterology. *Veterinary Clin North Am Exot Anim*
765 *Pract* **8**: 227–245.
766 Cole, K.D. and Little, G.H. (1983) Bile pigments and bilirubin UDP-glucuronyl transferase
767 during the metamorphosis of Rana catesbeiana tadpoles. *Comp Biochem Physiol B* **76**: 503–
768 506.
769 Colombo, B.M., Scalvenzi, T., Benlamara, S., and Pollet, N. (2015) Microbiota and mucosal
770 immunity in amphibians. *Front Immunol* **6**: 111.
771 Colston, T.J. and Jackson, C.R. (2016) Microbiome evolution along divergent branches of the
772 vertebrate tree of life: what is known and unknown. *Mol Ecol* **25**: 3776–3800.
773 Douglas, A.E. (2018) Fundamentals of Microbiome Science: How Microbes Shape Animal
774 Biology, Princeton: Princeton University Press.
775 Douglas, A.E. (2019) Simple animal models for microbiome research. *Nat Rev Microbiol* **17**:
776 764–775.
777 Escudie, F., Auer, L., Cauquil, L., Vidal, k., Maman, S., Mariadassou, M., et al. (July 6th to
778 9th) FROGS: Find Rapidly OTU with Galaxy Solution.
779 Faber, J. and Nieuwkoop, P.D. (1994) Normal Table of Xenopus Laevis, 1 edition. New
780 York: Garland Science.
781 Fedewa, L.A. (2006) Fluctuating Gram-Negative Microflora in Developing Anurans. *J*
782 *Herpetol* **40**: 131–135.
783 Frisch, K. and Alstrup, A.K.O. (2018) On the Evolution of Bile Salts and the Farnesoid X
784 Receptor in Vertebrates. *Physiol Biochem Zool PBZ* **91**: 797–813.
785 Funkhouser, L.J. and Bordenstein, S.R. (2013) Mom Knows Best: The Universality of
786 Maternal Microbial Transmission. *PLOS Biol* **11**: e1001631.
787 Gill, S.R., Pop, M., Deboy, R.T., Eckburg, P.B., Turnbaugh, P.J., Samuel, B.S., et al. (2006)
788 Metagenomic analysis of the human distal gut microbiome. *Science* **312**: 1355–1359.
789 Heimeier, R.A., Das, B., Buchholz, D.R., Fiorentino, M., and Shi, Y.-B. (2010) Studies on
790 Xenopus laevis intestine reveal biological pathways underlying vertebrate gut adaptation from
791 embryo to adult. *Genome Biol* **11**: R55.
792 Hird, S.M. (2017) Evolutionary Biology Needs Wild Microbiomes. *Front Microbiol* **8**: 725.

Hofmann, A.F., Hagey, L.R., and Krasowski, M.D. (2010) Bile salts of vertebrates: structural variation and possible evolutionary significance. *J Lipid Res* **51**: 226–246.
Hourdry, J., L'Hermite, A., and Ferrand, R. (1996) Changes in the Digestive Tract and Feeding Behavior of Anuran Amphibians during Metamorphosis. *Physiol Zool* **69**: 219–251.
Joyce, S.A., MacSharry, J., Casey, P.G., Kinsella, M., Murphy, E.F., Shanahan, F., et al. (2014) Regulation of host weight gain and lipid metabolism by bacterial bile acid modification in the gut. *Proc Natl Acad Sci U S A* **111**: 7421–7426.
Kohl, K.D., Cary, T.L., Karasov, W.H., and Dearing, M.D. (2013) Restructuring of the amphibian gut microbiota through metamorphosis. *Environ Microbiol Rep* **5**: 899–903.
Kopylova, E., Noé, L., and Touzet, H. (2012) SortMeRNA: fast and accurate filtering of ribosomal RNAs in metatranscriptomic data. *Bioinformatics* **28**: 3211–3217.
Long, J., Xiang, J., He, T., Zhang, N., and Pan, W. (2020) Gut microbiota differences during metamorphosis in sick and healthy giant spiny frogs (Paa spinosa) tadpoles. *Lett Appl Microbiol* **70**: 109–117.
Loudon, A.H., Woodhams, D.C., Parfrey, L.W., Archer, H., Knight, R., McKenzie, V., and Harris, R.N. (2014) Microbial community dynamics and effect of environmental microbial reservoirs on red-backed salamanders (Plethodon cinereus). *ISME J* **8**: 830–840.
Mashoof, S., Goodroe, A., Du, C.C., Eubanks, J.O., Jacobs, N., Steiner, J.M., et al. (2013) Ancient T-Independence of Mucosal IgX/A: Gut Microbiota Unaffected by Larval Thymectomy in Xenopus laevis. *Mucosal Immunol* **6**: 358–368.
Metchnikoff, O. (1901) Notes sur l'influence des microbes dans le développement des têtards. *Ann Inst Pasteur* **15**: 631–634.
Moro, E. (1905) Morphologische und biologische Untersuchungen über die Darmbakterien des Säuglings. IV. Der Schottelius's sche Versuch am Kalt- blutler. *Jahrb Kinderheilk* **62**: 467–478.
Naitoh, T., Wassersug, R.J., and Leslie, R.A. (1989) The Physiology, Morphology, and Ontogeny of Emetic behavior in Anuran amphibians. *Physiol Zool* **62**: 819–843.
Narayan, E.J. (2013) Non-invasive reproductive and stress endocrinology in amphibian conservation physiology. *Conserv Physiol* **1**: cot011.
Pasquier, L.D. (2014) The Development of the Immune System in Xenopus. In *Xenopus Development*. Kloc, lgorzata and Kubiak, J.Z. (eds). John Wiley & Sons, Inc, pp. 264–292.
Powell, S., Forslund, K., Szklarczyk, D., Trachana, K., Roth, A., Huerta-Cepas, J., et al. (2014) eggNOG v4.0: nested orthology inference across 3686 organisms. *Nucleic Acids Res* **42**: D231-239.
Pryor, G.S. and Bjorndal, K.A. (2005) Symbiotic fermentation, digesta passage, and gastrointestinal morphology in bullfrog tadpoles (Rana catesbeiana). *Physiol Biochem Zool* **78**: 201–215.
R Core Team (2019) R: A language and environment for statistical computing.
Rebollar, E.A. and Harris, R.N. (2019) Editorial: Ecology of Amphibian-Microbial Symbioses. *Front Microbiol* **10**:.
Reschly, E.J., Ai, N., Ekins, S., Welsh, W.J., Hagey, L.R., Hofmann, A.F., and Krasowski, M.D. (2008) Evolution of the bile salt nuclear receptor FXR in vertebrates. *J Lipid Res* **49**: 1577–1587.
Ridlon, J.M., Kang, D.J., Hylemon, P.B., and Bajaj, J.S. (2014) Bile Acids and the Gut Microbiome. *Curr Opin Gastroenterol* **30**: 332–338.
Robert, J. and Ohta, Y. (2009) Comparative and developmental study of the immune system in Xenopus. *Dev Dyn* **238**: 1249–1270.
Rollins-Smith, L.A., Barker, K.S., and Davis, A.T. (1997) Involvement of glucocorticoids in the reorganization of the amphibian immune system at metamorphosis. *Dev Immunol* **5**: 145–152.

Sachs, L.M. and Buchholz, D.R. (2019) Insufficiency of Thyroid Hormone in Frog Metamorphosis and the Role of Glucocorticoids. *Front Endocrinol* **10**: 287.
Schreiber, A.M., Cai, L., and Brown, D.D. (2005) Remodeling of the intestine during metamorphosis of Xenopus laevis. *Proc Natl Acad Sci U S A* **102**: 3720–3725.
Seemann, T. (2014) Prokka: rapid prokaryotic genome annotation. *Bioinforma Oxf Engl* **30**: 2068–2069.
Sekirov, I., Russell, S.L., Antunes, L.C.M., and Finlay, B.B. (2010) Gut microbiota in health and disease. *Physiol Rev* **90**: 859–904.
Seo, Y.-W., Sanyal, S., Kim, H.-J., Won, D.H., An, J.-Y., Amano, T., et al. (2002) FOR, a Novel Orphan Nuclear Receptor Related to Farnesoid X Receptor. *J Biol Chem* **277**: 17836–17844.
Shenhav, L., Thompson, M., Joseph, T.A., Briscoe, L., Furman, O., Bogumil, D., et al. (2019) FEAST: fast expectation-maximization for microbial source tracking. *Nat Methods* **16**: 627–632.
Sommer, F. and Bäckhed, F. (2013) The gut microbiota--masters of host development and physiology. *Nat Rev Microbiol* **11**: 227–238.
Song, Z., Cai, Y., Lao, X., Wang, X., Lin, X., Cui, Y., et al. (2019) Taxonomic profiling and populational patterns of bacterial bile salt hydrolase (BSH) genes based on worldwide human gut microbiome. *Microbiome* **7**: 9.
Vences, M., Lyra, M.L., Kueneman, J.G., Bletz, M.C., Archer, H.M., Canitz, J., et al. (2016) Gut bacterial communities across tadpole ecomorphs in two diverse tropical anuran faunas. *Naturwissenschaften* **103**: 25.
Vouillot, L., Thélie, A., Scalvenzi, T., and Pollet, N. (2014) Genomics and Genome Engineering in Xenopus. In *Xenopus Development*. Kloc, lgorzata and Kubiak, J.Z. (eds). John Wiley & Sons, Inc, pp. 383–402.
Wahlström, A., Sayin, S.I., Marschall, H.-U., and Bäckhed, F. (2016) Intestinal Crosstalk between Bile Acids and Microbiota and Its Impact on Host Metabolism. *Cell Metab* **24**: 41–50.
Walke, J.B., Becker, M.H., Loftus, S.C., House, L.L., Cormier, G., Jensen, R.V., and Belden, L.K. (2014) Amphibian skin may select for rare environmental microbes. *ISME J* **8**: 2207–2217.
Wang, Q., Garrity, G.M., Tiedje, J.M., and Cole, J.R. (2007) Naive Bayesian classifier for rapid assignment of rRNA sequences into the new bacterial taxonomy. *Appl Environ Microbiol* **73**: 5261–5267.
Warne, R.W., Kirschman, L., and Zeglin, L. (2019) Manipulation of gut microbiota during critical developmental windows affects host physiological performance and disease susceptibility across ontogeny. *J Anim Ecol* **88**: 845–856.
Warne, R.W., Kirschman, L., and Zeglin, L. (2017) Manipulation of Gut Microbiota Reveals Shifting Community Structure Shaped by Host Developmental Windows in Amphibian Larvae. *Integr Comp Biol* **57**: 786–794.
Watanabe, M., Houten, S.M., Mataki, C., Christoffolete, M.A., Kim, B.W., Sato, H., et al. (2006) Bile acids induce energy expenditure by promoting intracellular thyroid hormone activation. *Nature* **439**: 484–489.
Wilson, D.S. and Sober, E. (1989) Reviving the superorganism. *J Theor Biol* **136**: 337–356.
Wollman, E. (1913) Sur l'élevage des têtards stériles. *Ann Inst Pasteur* **27**: 154–161.
Wollman, E. and Wollman, E. (1915) Les microbes dans l'alimentation des têtards. *Compte-Rendu Société Biol* **78**: 195–197.
Xiao, L., Feng, Q., Liang, S., Sonne, S.B., Xia, Z., Qiu, X., et al. (2015) A catalog of the mouse gut metagenome. *Nat Biotechnol*.
Youngblut, N.D., Reischer, G.H., Walters, W., Schuster, N., Walzer, C., Stalder, G., et al.

893 (2019) Host diet and evolutionary history explain different aspects of gut microbiome
894 diversity among vertebrate clades. *Nat Commun* **10**: 2200.
895 Zhang, M., Chen, H., Liu, L., Xu, L., Wang, X., Chang, L., et al. (2020) The Changes in the
896 Frog Gut Microbiome and Its Putative Oxygen-Related Phenotypes Accompanying the
897 Development of Gastrointestinal Complexity and Dietary Shift. *Front Microbiol* **11**: 162.
898 Zilber-Rosenberg, I. and Rosenberg, E. (2008) Role of microorganisms in the evolution of
899 animals and plants: the hologenome theory of evolution. *FEMS Microbiol Rev* **32**: 723–735.
900

901 # Figure legends

902 **Figure 1**: **Enumeration of bacteria in the *Xenopus tropicalis* gut during development.**

903 **A. Cytometric profiles**. Each dot in the plot represent one event (i.e. a cell), the color represents
904 the density of overlapping point from red to blue. The vertical axis represents the measurement
905 of propidium iodide (PI) fluorescence (614/20nm) and the horizontal axis represents the
906 measurement of forward scatter. The two plots represent the result for young tadpole at stage
907 NF45-48 (top) and mature tadpoles at stage NF56 (bottom). White letters highlight the different
908 bacterial population. The signal at around 10 units of fluorescence is due to background. **B.**
909 **Changes of bacterial load during development**. The vertical axis represents the number of
910 bacteria and the horizontal axis corresponds to the different stages of development. Each dot
911 corresponds to a biological replicate, the error bar represents the standard deviation obtained
912 by technical replicates. A ★ marks the beginning of feeding and ★★ marks the change from
913 the tadpole to the adult diet.

914 **Figure 2: Bacterial communities in the Xenopus gut across development.**

915 **A. Bar plot representation of the bacterial diversity at the phylum level**. Tad:
916 premetamorphic tadpoles NF54 to NF56. Pro: prometamorphic tadpoles NF58 to NF61; Met:
917 Metamorphic tadpole NF 62; Fro: Froglet NF66; Adu: sexually mature adults. **B. Microbiota**
918 **diversity during Xenopus development.** Phylogenetic diversity measured using Faith' PD
919 index for *X. tropicalis* gut microbial communities across developmental life stages as indicated

920 on the x-axis. Letters a, b and c indicate significant differences at the 0.05 level between
921 developmental stages according to pairwise Dunn's rank sum post-hoc test (see Methods
922 section for details). **C. Principal coordinate analysis of gut-associated microbial**
923 **communities during Xenopus development.** Community membership was analyzed using
924 unweighted UniFrac distance, and community structure was analyzed using philR distance.
925 Percentages of the explained variations are indicated on both axes.
926
927 **Figure 3: *Xenopus* microbiota across several adult organs and samples**
928 **A. Bar plot representation of the bacterial phylum diversity**. **B. Principal coordinate**
929 **analysis of microbial communities across several adult organs and samples.** Community
930 membership was analyzed using unweighted UniFrac distance, and community structure was
931 analyzed using weighted UniFrac distance. Percentages of the explained variations are
932 indicated on both axes.
933
934 **Figure 4: Characterization of the prevalence and abundances of active bacteria across**
935 **Xenopus development from post-hatching to metamorphosis.**
936 **A. Heatmap of the prevalence and abundances for 33 OTUs**. The detection threshold scale
937 is logarithmic and the metric used was the relative abundance. OTUs were identified using their
938 taxonomic affiliation at the family genus or species level according to the resolution available
939 for a given OTU. This analysis was performed on OTUs characterized by a minimal prevalence
940 of 50 % and a minimal abundance of 0.001%.
941 **B. Abundance heatmap for the 33 most prevalent OTUs across the developmental stages**
942 **sampled.** Two clutches were followed up across development, and the white dotted lines
943 separate the two biological replicate samples. The legend for stages is as follows: PE is a post-
944 hatching NF30 tailbud embryonic stage; NF41 is a premetamorphic tadpole non-feeding stage;

945 NF48 is a premetamorphic tadpole feeding stage; NF50; NF 52 and NF56 are premetamorphic
946 tadpole feeding stages; NF60 is a prometamorphic tadpole stage; NF63 are metamorphic
947 tadpole stages; NF66 is a froglet stage.

948 **Figure 5: Influence of the tadpole's diet on their gut microbiome.**

949 **A. Bar plot representation of the bacterial phylum diversity**. **B. Principal coordinate**
950 **analysis of microbial communities across several adult organs and samples.** Community
951 membership was analyzed using unweighted UniFrac distance, and community structure was
952 analyzed using weighted UniFrac distance. Percentages of the explained variations are
953 indicated on both axes. Tadpole Food 1 (D1 samples) was a micro planktonic-based diet and
954 tadpole food 2 (D2 samples) (food 1) was a sterile flour.

955

956 **Figure 6: *X. tropicalis* microbiome transmission**

957 **A. Bar plot representation of the bacterial phylum diversity.**

958 **B. Box-plot representation of weighted UniFrac distances between eggs, skin and feces.**
959 Letters a, b and c indicate significant differences at the 0.05 level between or within samples
960 according to pairwise Dunn's rank sum post-hoc test (see Methods section for details). Note
961 the outliers in the feces sample and in the Eggs-skin comparison.

962 **C. Bar plot representation of source proportions in egg microbiomes.**

963 **D. Principal coordinate analysis of microbial communities across eggs, feces and skin**
964 **samples.** Community composition was analyzed using PhilR distance. Percentages of the
965 explained variations are indicated on both axes.

966

967 **Figure 7**: **Bacterial taxonomic profiles from *X. tropicalis* prometamorphic tadpole gut. A.**
968 Histogram representation of the bacterial phylum diversity observed in a pool of five
969 prometamorphic tadpole's guts at stage NF56. Left: metagenomic analysis; right:

970 metatranscriptomic analysis. Each color in the histogram refers to the phylum as described in
971 the legend. Phyla representing less than one percent of the bacterial content in the tadpole gut
972 were represented in the "Other group". **B.** Abundance of the most abundant bacteria in the
973 tadpole's gut. Bacteria representing less than one percent of the bacterial population were
974 represented in the "Other" group. The abundance of each bacteria is given as the percentage of
975 the total bacteria. Bacteria species written in blue, orange or grey correspond to bacteria
976 observed in human gut microbiota, other mammalian gut microbiota or endosymbiotic bacteria
977 of unicellular eukaryotes, respectively.
978
979 **Figure 8**: **Overview of *X. tropicalis* tadpole's microbiota metabolic functions.** Histogram
980 representing the distribution of the *Xenopus* gut metagenome CDS among the eggNOG
981 functional categories. The black histogram represents the distribution expressed as the
982 percentage of the total number of CDS. The grey histogram represents the expression value for
983 each eggnog category expressed as the percentage of the total expression.
984 **Supplementary data R scripts: R markdown rendered html files**
985
986 **Additional files:**
987 **Additional file 1: Supplementary_table_1.csv**
988 File format: csv
989 Title of data: Metadata.
990 Description of data: This file contains the metadata corresponding to samples analysed by 16S
991 rRNA gene metabarcoding.
992
993 **Additional file 2: Table_Statistics**
994 File format: xlsx

995 Title of data: Compilation of statistical results in tables.

996 Description of data: This file contains seven tables compiling the results of significance tests

997 for alpha and beta diversity metrics.

998

999 **Additional file 3: Figure_S1**

1000 File format: pdf

1001 Title of data: Results of flow cytometry across developmental stages.

1002 Description of data: Cytometric profiles obtained at different stages of tadpole's development.

1003 Each dot in the plot represents a cell; the color represents the density of overlapping point from

1004 red to blue. A: Vertical axis represents the measurement of fluorescence (propidium iodide -

1005 614/20nm) and the horizontal axis the measurement of forward scatter. B: Vertical axis

1006 represents the measurement of propidium iodide (PI) fluorescence (614/20nm) and the

1007 horizontal axis the measurement of side scatter. The black circles highlight the beads used for

1008 calibration.

1009

1010 **Additional file 4: Figure_S2**

1011 File format: pdf

1012 Title of data: Rarefaction curve analysis.

1013 Description of data: This graph present rarefaction curves for all samples studied in this

1014 analysis.

1015

1016 **Additional file 5: Figure_S3**

1017 File format: pdf

1018 Title of data: Phylum and Family-level compositional changes in the *Xenopus* gut microbiome

1019 across development.

1020 Description of data: A: Bar plot representation of the bacterial diversity at the phylum level. B:
1021 Bar plot representation of the bacterial diversity at the family level. Premetamorphic tadpoles
1022 NF54 to NF56. Prometamorphic tadpoles NF58 to NF61; Metamorphic tadpole NF 62; Froglet
1023 NF66; Adult: sexually mature adults. C: Same as A but viewed at the individual level to
1024 highlight the interindividual and developmental stage differences D: Bar plot representation of
1025 gram positive and gram negative bacterial phyla.
1026
1027 **Additional file 6: Figure_S4**
1028 File format: pdf
1029 Title of data: Shared and contrasting bacterial communities in the Xenopus gut microbiome
1030 across development.
1031 Description of data: A : Venn diagram showing the number of shared OTUs between samples
1032 of the same developmental stage category. B : Bar plot of the total number of OTUs in each
1033 developmental stage category. C : Number of shared and specific OTUs. D : Heatmap plot of
1034 the prevalence and abundances for low-abundance OTUs. The detection threshold scale is
1035 logarithmic and the metric used was the relative abundance. This analysis was performed on
1036 OTUs characterized by a minimal prevalence of 50 % and a minimal abundance of 1e-5 %. E.
1037 Prevalence and abundances of the most common and the most abundant OTUs across
1038 development. OTUs were identified using their taxonomic affiliation at the family genus or
1039 species level according to the resolution available for a given OTU. This analysis was
1040 performed on OTUs characterized by a minimal prevalence of 50 % and a minimal abundance
1041 of 0.001%. The right panel shows an abundance heatmap for the same OTUs to visualize their
1042 abundances in each sample.
1043
1044 **Additional file 7: Figure_S5**

1045 File format: pdf

1046 Title of data: Contrasting OTUs across development

1047 Description of data: A : Abundance fold changes across development. Contrasting OTUs were
1048 identied by filtering OTUs with an abundance of at least 100 reads across 20% of sample and
1049 using DEseq2 with a significance cutoff of 0.01. B : Heatmap representation of contrasting
1050 OTUs abundances across development. The heatmap was produced using a principal
1051 component analysis based on UniFrac distances.

1052

1053 **Additional file 8: Figure_S6**

1054 File format: pdf

1055 Title of data: Variations of the phylogenetic structure of the *Xenopus* gut microbiota during
1056 development.

1057 Description of data: Standardized effect sizes of the Mean pairwise distance (left panel) and of
1058 the mean nearest taxon distance (right panel) measured using Faith' PD index for *X. tropicalis*
1059 gut microbial communities across developmental life stages as indicated on the x-axis. Letters
1060 a, b and c indicate significant differences at the 0.05 level between developmental stages
1061 according to pairwise Dunn's rank sum post-hoc test (see Methods section for details).

1062

1063 **Additional file 9: Figure_S7**

1064 File format: pdf

1065 Title of data: *Xenopus* tadpole active bacterial communities: alpha-diversity, bacterial phylum
1066 diversity and source proportions

1067 Description of data: A : Bar plot representation of OTU richness and phylogenetic diversity in
1068 active bacterial communities. Two clutches were followed up across early development, and
1069 the light and dark grey bars correspond to the two biological replicate samples. The legend for

1070 stages is as follows: NF30 is a post-hatching tailbud embryonic stage; NF41 is a
1071 premetamorphic tadpole non-feeding stage; NF48 is a premetamorphic tadpole feeding stage;
1072 NF50 and NF 52 are premetamorphic tadpole feeding stages. B : Bar plot representation of the
1073 bacterial phylum diversity. C : Bar plot representation of source proportions in froglet gut
1074 microbiome.
1075
1076 **Additional file 10: Figure_S8**
1077 File format: pdf
1078 Title of data: Impact of the food regime on tadpole growth and development.
1079 Description of data: A: Impact of food diet on tadpole growth and development. Tadpoles were
1080 fed using either a micro planktonic-based diet (food 1) or a sterile flour (food 2). Their growth
1081 was assessed by weighting them, and their development was monitored by assessing their
1082 developmental stage according to the Nieuwkoop and Faber developmental table. The food
1083 regime did not change significantly tadpole growth (Kruskal-Wallis chi-squared = 0.99, df = 1,
1084 p = 0.32) or development (Kruskal-Wallis chi-squared = 0.34, df = 1, p = 0.56). B : Impact of
1085 the food regime on tadpole's guts microbial communities. These bar plot shows values of the
1086 Standardized effect size of the Mean Pairwise Distance (SES MPD) and of the Mean Nearest
1087 Taxon Distance (SES MNTD) according to the food regime given to groups of tadpoles. C :
1088 Abundance ratios of the OTUs found significantly different according to a change of diet.
1089
1090 **Additional file 11: Figure_S9**
1091 File format: pdf
1092 Title of data: GC percent analysis of the ten longest metagenomic scaffolds.
1093 Description of data: Vertical axis represents the GC percent and horizontal axis the position on
1094 the scaffold in base pair (bp). GC percent was computed for a sliding window of 2,000bp.

1095

1096 **Additional file 12: Figure_S10**

1097 File format: pdf

1098 Title of data: Reads coverage of the ten longest metagenomic scaffolds.

1099 Description of data: The number of reads aligned on the ten longest scaffolds is presented on

1100 the vertical axis with a logarithmic scale, the horizontal axis represents the position on the

1101 scaffold in base pair (bp).

1102

1103 **Additional file 13: Figure_S11**

1104 File format: pdf

1105 Title of data: Metabolic map of *X. tropicalis* genome and its gut metagenome.

1106 Description of data: This metabolic pathway highlights in green the pathways shared between

1107 the *Xenopus* genome and its gut metagenome. Red and blue pathways are unique to the *Xenopus*

1108 genome and gut metagenome, respectively.

1109

1110 **Additional file 12: Extended_materials_and_methods**

1111 File format: docx

1112 Title of data: Extended materials and methods.

1113 Description of data: This file contains an extended version of the materials and methods

1114

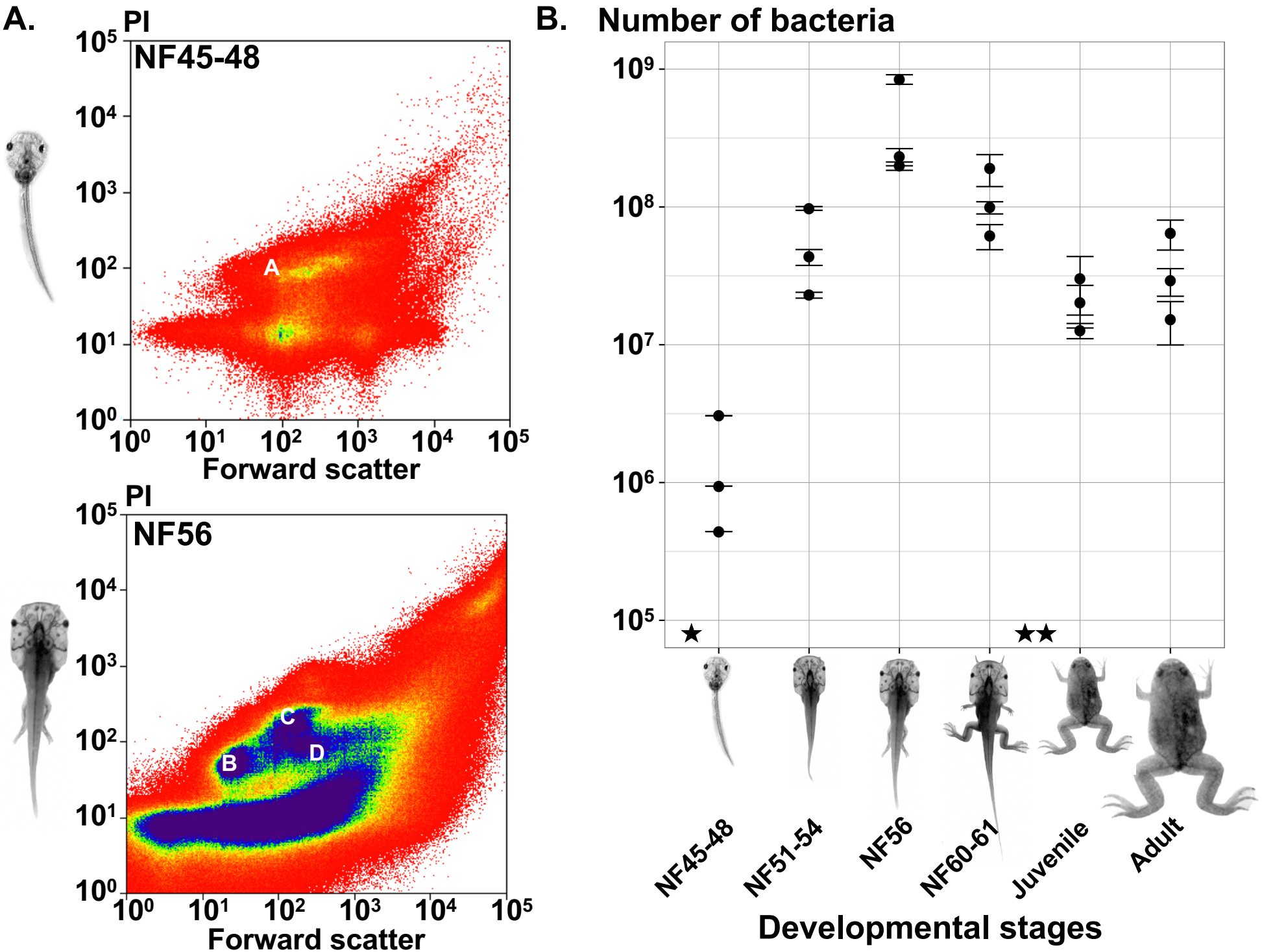
A.
PI
NF45-48
A
Forward scatter
PI
NF56
B
C
D
Forward scatter
B.
Number of bacteria
NF45-48
NF51-54
NF56
NF60-61
Juvenile
Adult
Developmental stages

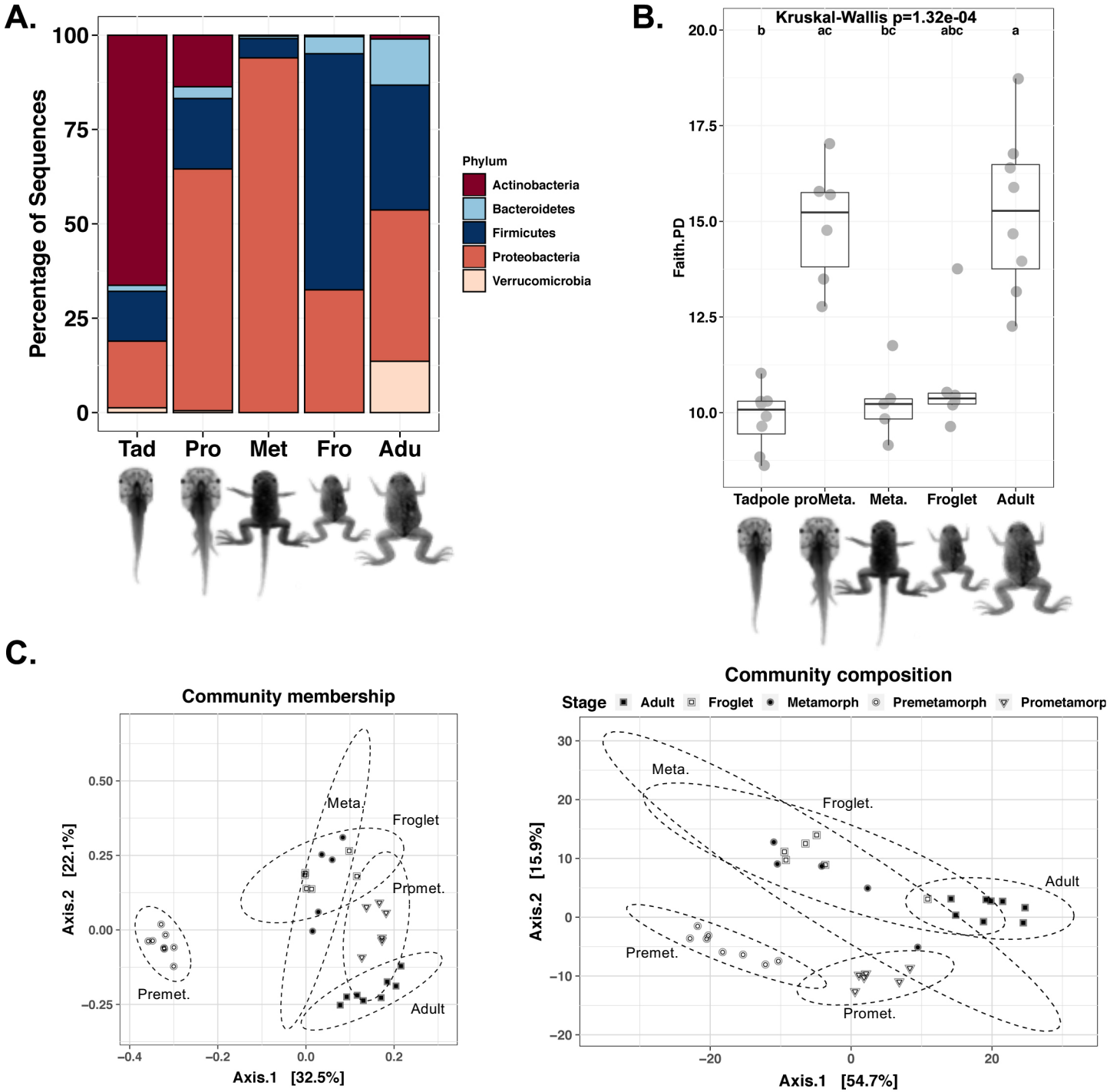
A.
Percentage of Sequences
100
75
50
25
0
Tad
Pro
Met
Fro
Adu
Phylum
Actinobacteria
Bacteroidetes
Firmicutes
Proteobacteria
Verrucomicrobia
B.
Kruskal-Wallis p=1.32e-04
b
ac
bc
abc
a
Faith.PD
20.0
17.5
15.0
12.5
10.0
Tadpole
proMeta.
Meta.
Froglet
Adult
C.
Community membership
Axis.2 [22.1%]
0.50
0.25
0.00
−0.25
−0.4
−0.2
0.0
0.2
Axis.1 [32.5%]
Meta.
Froglet
Prpmet.
Premet.
Adult
Community composition
Stage
Adult
Froglet
Metamorph
Premetamorph
Prometamorp
Axis.2 [15.9%]
30
20
10
0
−10
−20
−20
0
20
Axis.1 [54.7%]
Meta.
Froglet.
Adult
Premet.
Promet.

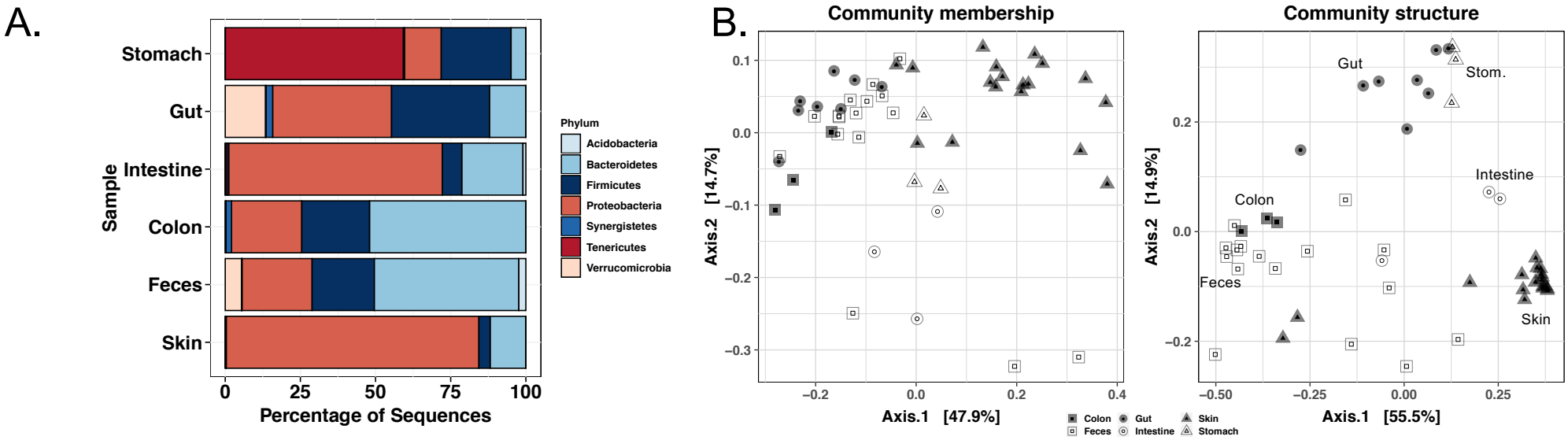
A.
Stomach
Gut
Intestine
Colon
Feces
Skin
Sample
0
25
50
75
100
Percentage of Sequences
Phylum
Acidobacteria
Bacteroidetes
Firmicutes
Proteobacteria
Synergistetes
Tenericutes
Verrucomicrobia
B.
Community membership
Community structure
Axis.2 [14.7%]
Axis.1 [47.9%]
Axis.2 [14.9%]
Axis.1 [55.5%]
Gut
Stom.
Intestine
Colon
Feces
Skin
Colon
Feces
Gut
Intestine
Skin
Stomach

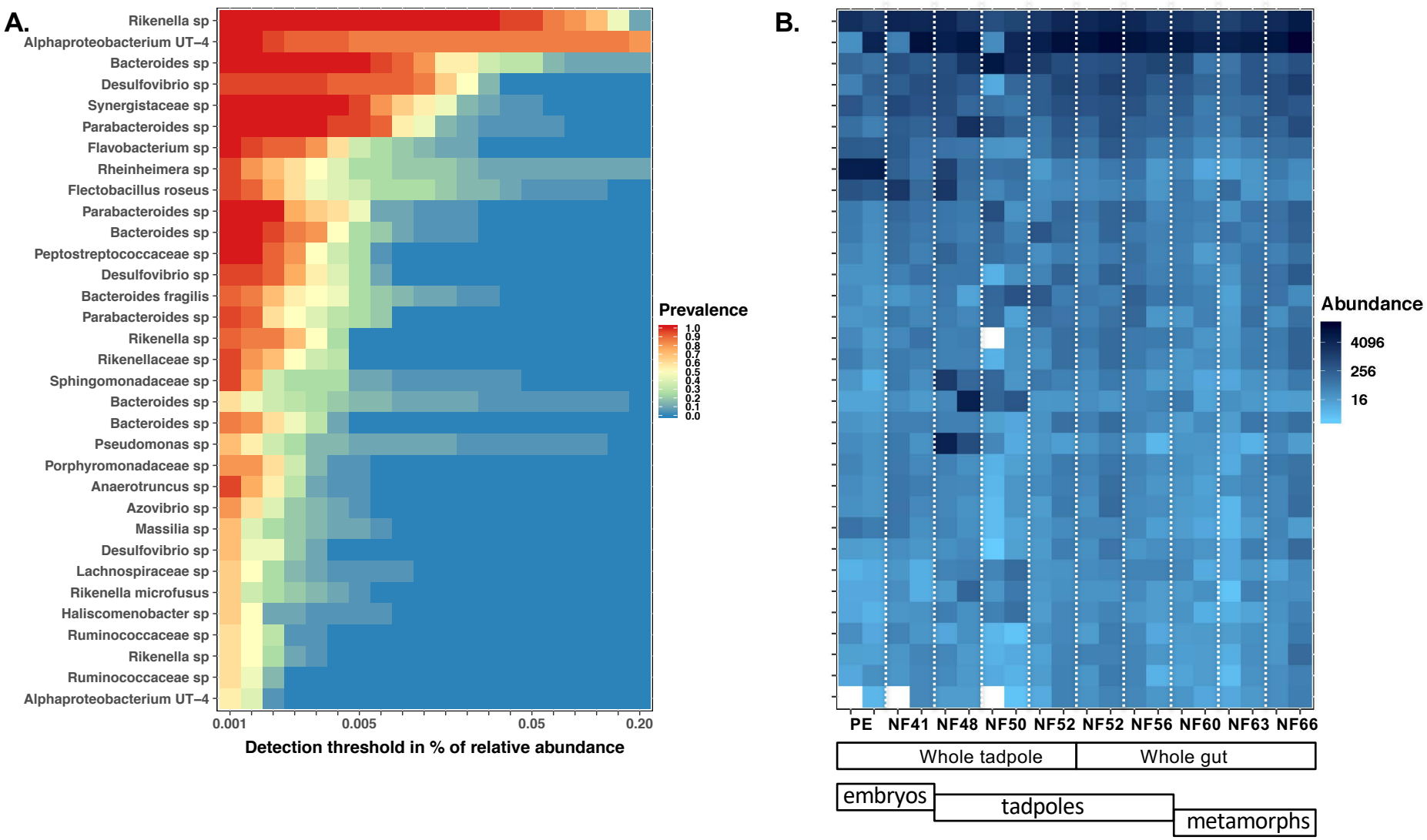
A.
Rikenella sp
Alphaproteobacterium UT−4
Bacteroides sp
Desulfovibrio sp
Synergistaceae sp
Parabacteroides sp
Flavobacterium sp
Rheinheimera sp
Flectobacillus roseus
Parabacteroides sp
Bacteroides sp
Peptostreptococcaceae sp
Desulfovibrio sp
Bacteroides fragilis
Parabacteroides sp
Rikenella sp
Rikenellaceae sp
Sphingomonadaceae sp
Bacteroides sp
Bacteroides sp
Pseudomonas sp
Porphyromonadaceae sp
Anaerotruncus sp
Azovibrio sp
Massilia sp
Desulfovibrio sp
Lachnospiraceae sp
Rikenella microfusus
Haliscomenobacter sp
Ruminococcaceae sp
Rikenella sp
Ruminococcaceae sp
Alphaproteobacterium UT−4
0.001
0.005
0.05
0.20
Detection threshold in % of relative abundance
Prevalence
1.0
0.9
0.8
0.7
0.6
0.5
0.4
0.3
0.2
0.1
0.0
B.
PE
NF41
NF48
NF50
NF52
NF52
NF56
NF60
NF63
NF66
Whole tadpole
Whole gut
embryos
tadpoles
metamorphs
Abundance
4096
256
16

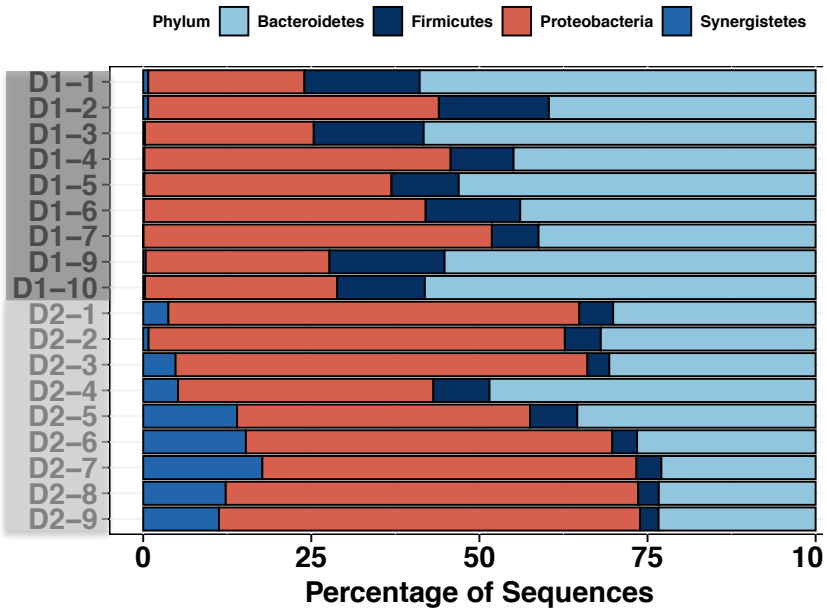
Phylum
Bacteroidetes
Firmicutes
Proteobacteria
Synergistetes
D1−1
D1−2
D1−3
D1−4
D1−5
D1−6
D1−7
D1−9
D1−10
D2−1
D2−2
D2−3
D2−4
D2−5
D2−6
D2−7
D2−8
D2−9
0
25
50
75
10
Percentage of Sequences

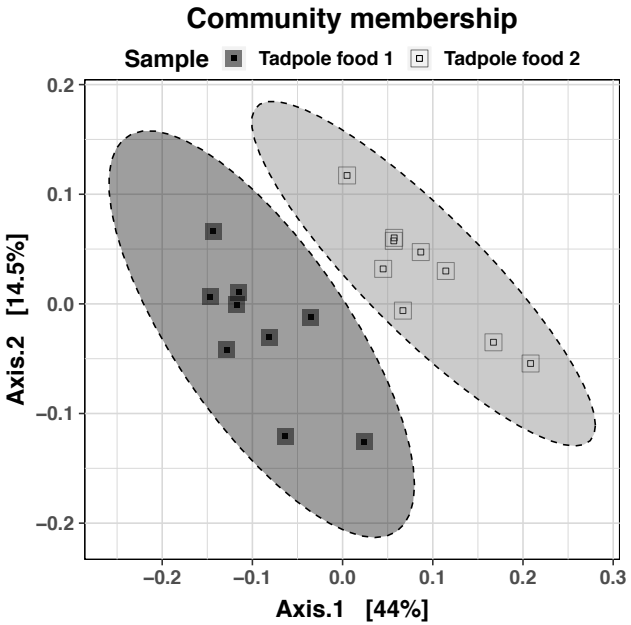
Community membership
Sample
Tadpole food 1
Tadpole food 2
Axis.2 [14.5%]
Axis.1 [44%]
0.2
0.1
0.0
−0.1
−0.2
−0.2
−0.1
0.0
0.1
0.2
0.3

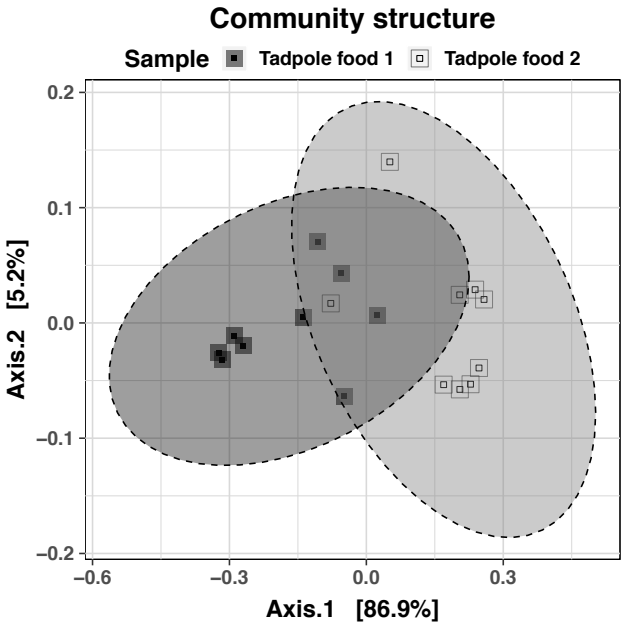
Community structure
Sample
Tadpole food 1
Tadpole food 2
Axis.2 [5.2%]
Axis.1 [86.9%]
0.2
0.1
0.0
−0.1
−0.2
−0.6
−0.3
0.0
0.3

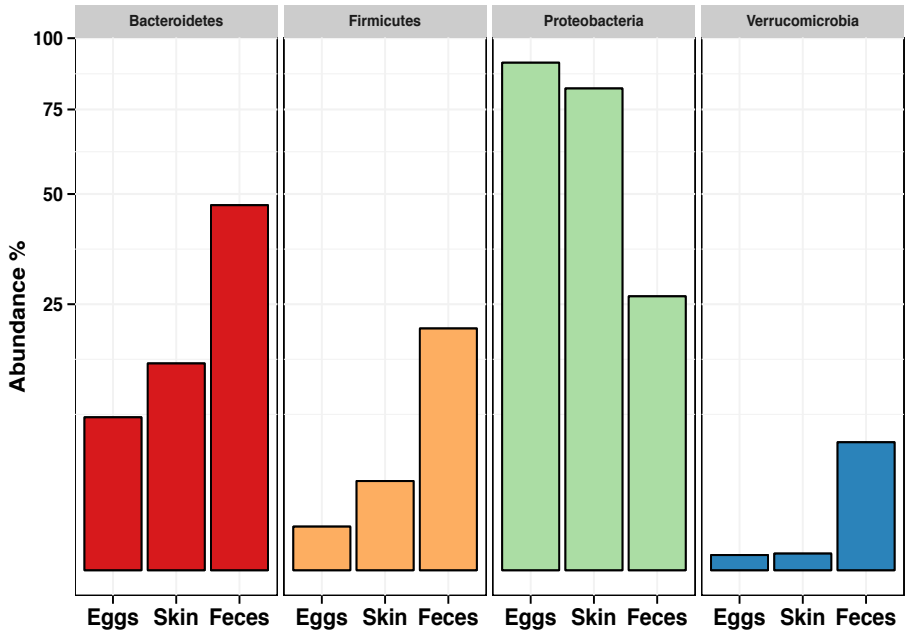
Bacteroidetes
Firmicutes
Proteobacteria
Verrucomicrobia
Abundance %
100
75
50
25
Eggs Skin Feces
Eggs Skin Feces
Eggs Skin Feces
Eggs Skin Feces

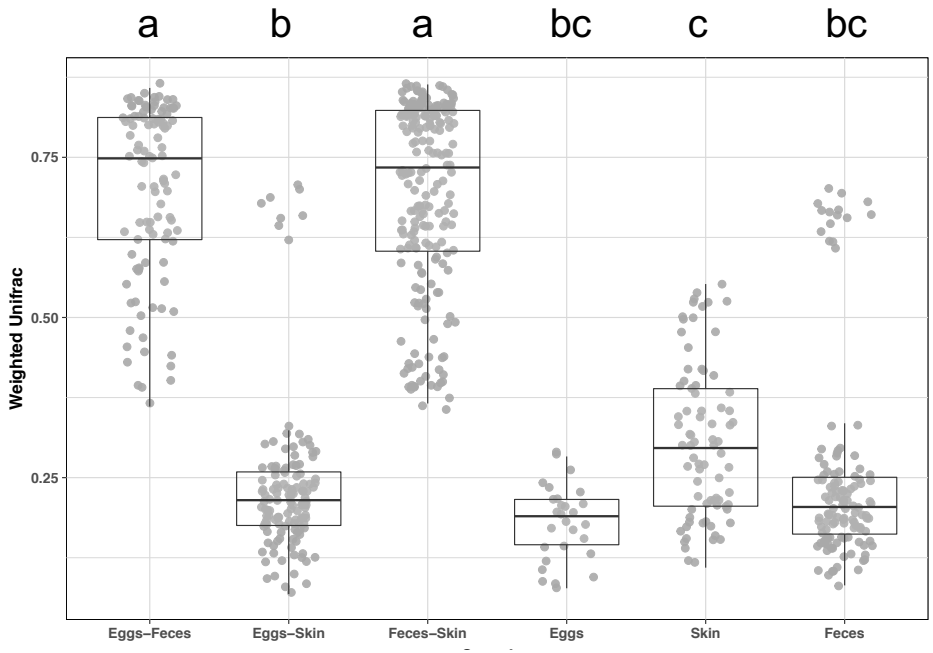
a b a bc c bc
Weighted Unifrac
0.75
0.50
0.25
Eggs–Feces
Eggs–Skin
Feces–Skin
Eggs
Skin
Feces

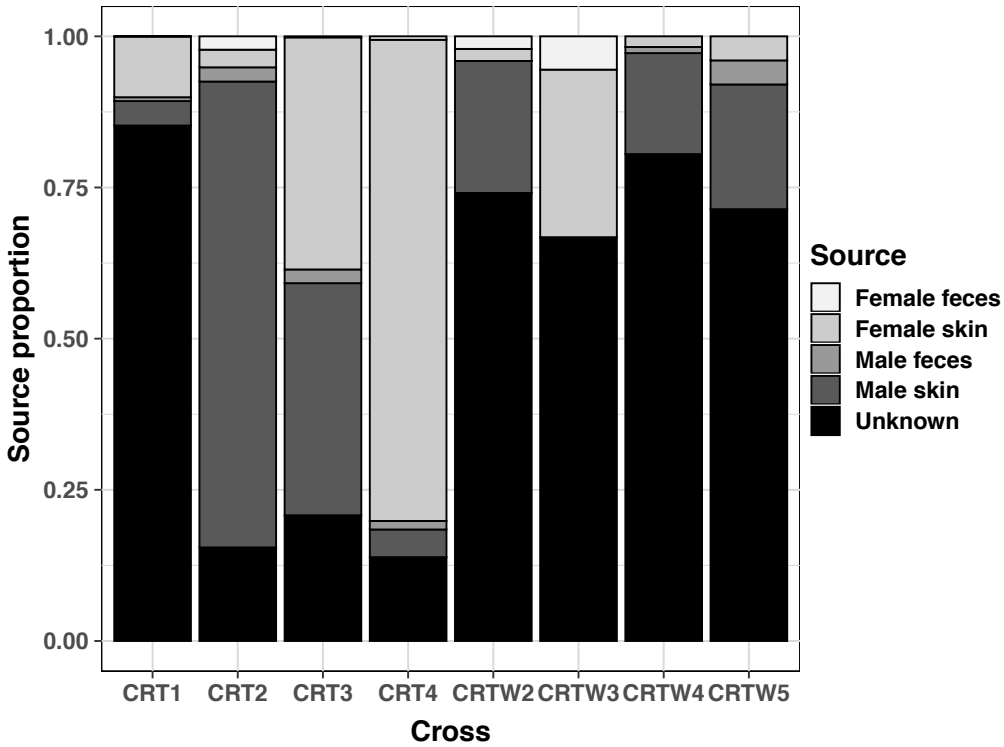
Source proportion
1.00
0.75
0.50
0.25
0.00
CRT1 CRT2 CRT3 CRT4 CRTW2 CRTW3 CRTW4 CRTW5
Cross
Source
Female feces
Female skin
Male feces
Male skin
Unknown

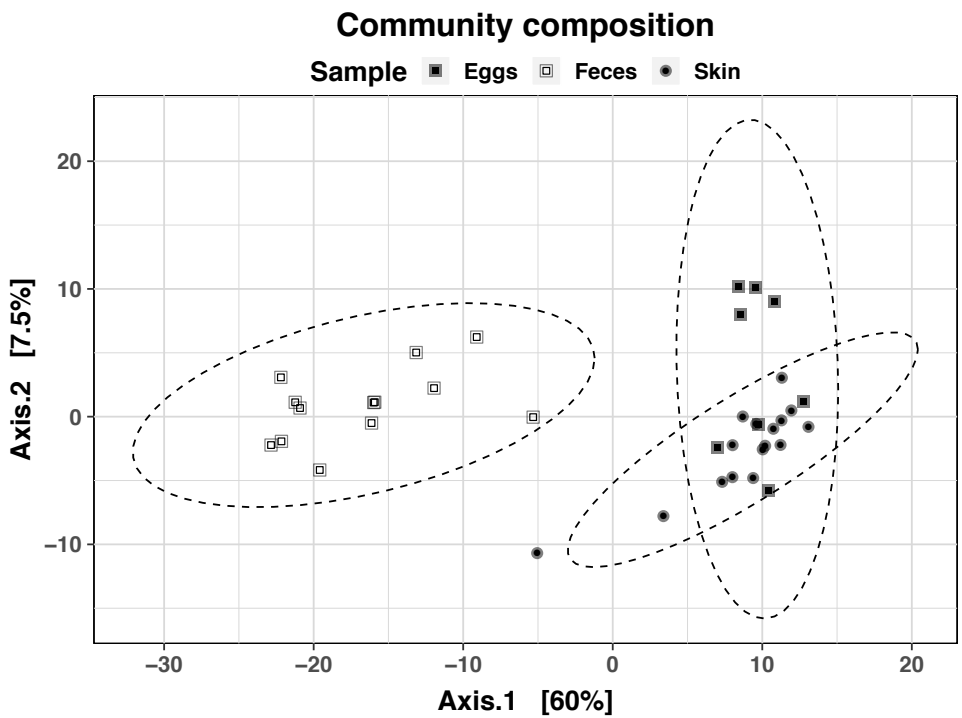
Community composition
Sample Eggs Feces Skin
Axis.2 [7.5%]
20
10
0
−10
−30 −20 −10 0 10 20
Axis.1 [60%]

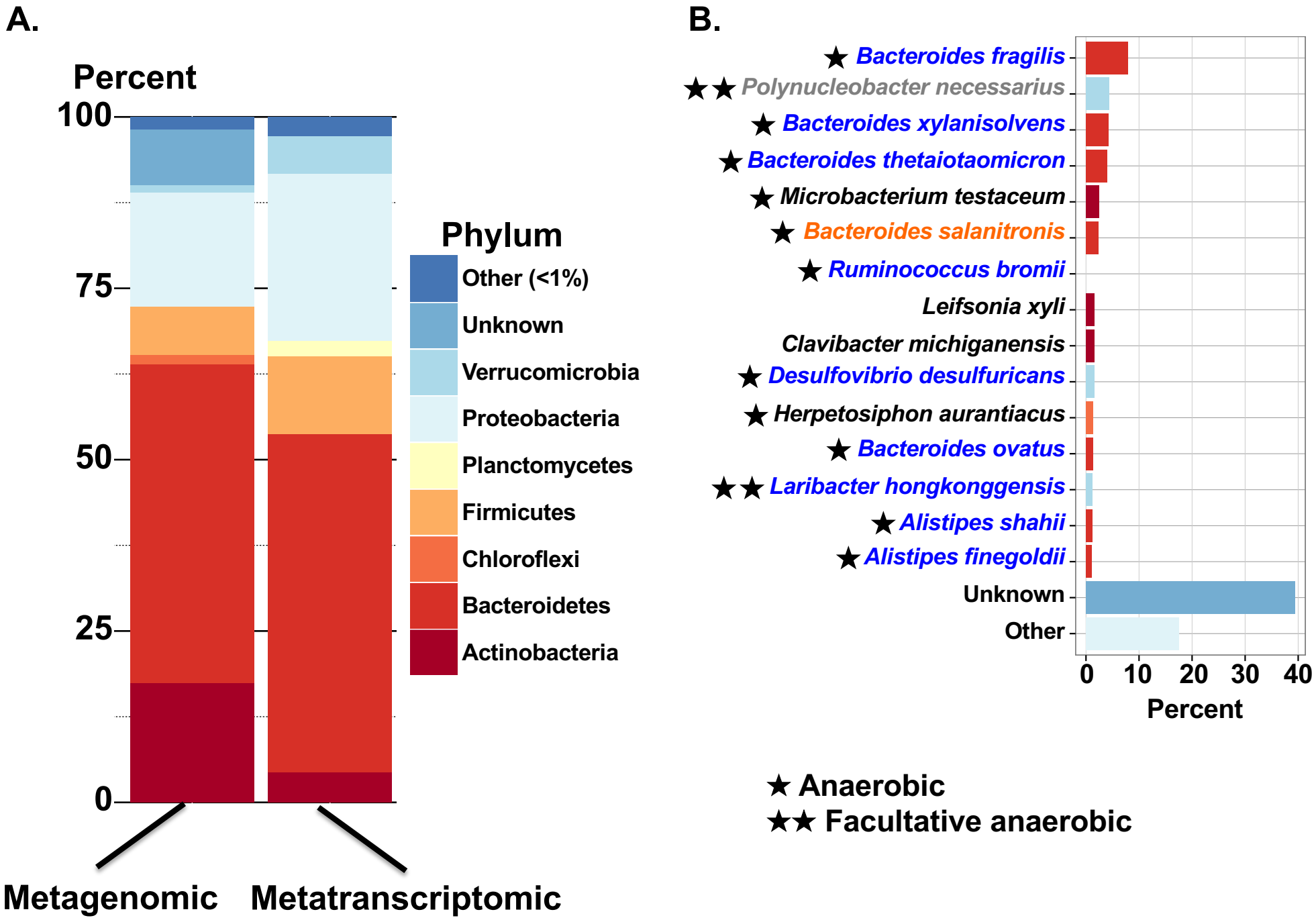
A.
Percent
100
75
50
25
0
Phylum
Other (<1%)
Unknown
Verrucomicrobia
Proteobacteria
Planctomycetes
Firmicutes
Chloroflexi
Bacteroidetes
Actinobacteria
Metagenomic
Metatranscriptomic
B.
Bacteroides fragilis
Polynucleobacter necessarius
Bacteroides xylanisolvens
Bacteroides thetaiotaomicron
Microbacterium testaceum
Bacteroides salanitronis
Ruminococcus bromii
Leifsonia xyli
Clavibacter michiganensis
Desulfovibrio desulfuricans
Herpetosiphon aurantiacus
Bacteroides ovatus
Laribacter hongkonggensis
Alistipes shahii
Alistipes finegoldii
Unknown
Other
0
10
20
30
40
Percent
Anaerobic
Facultative anaerobic

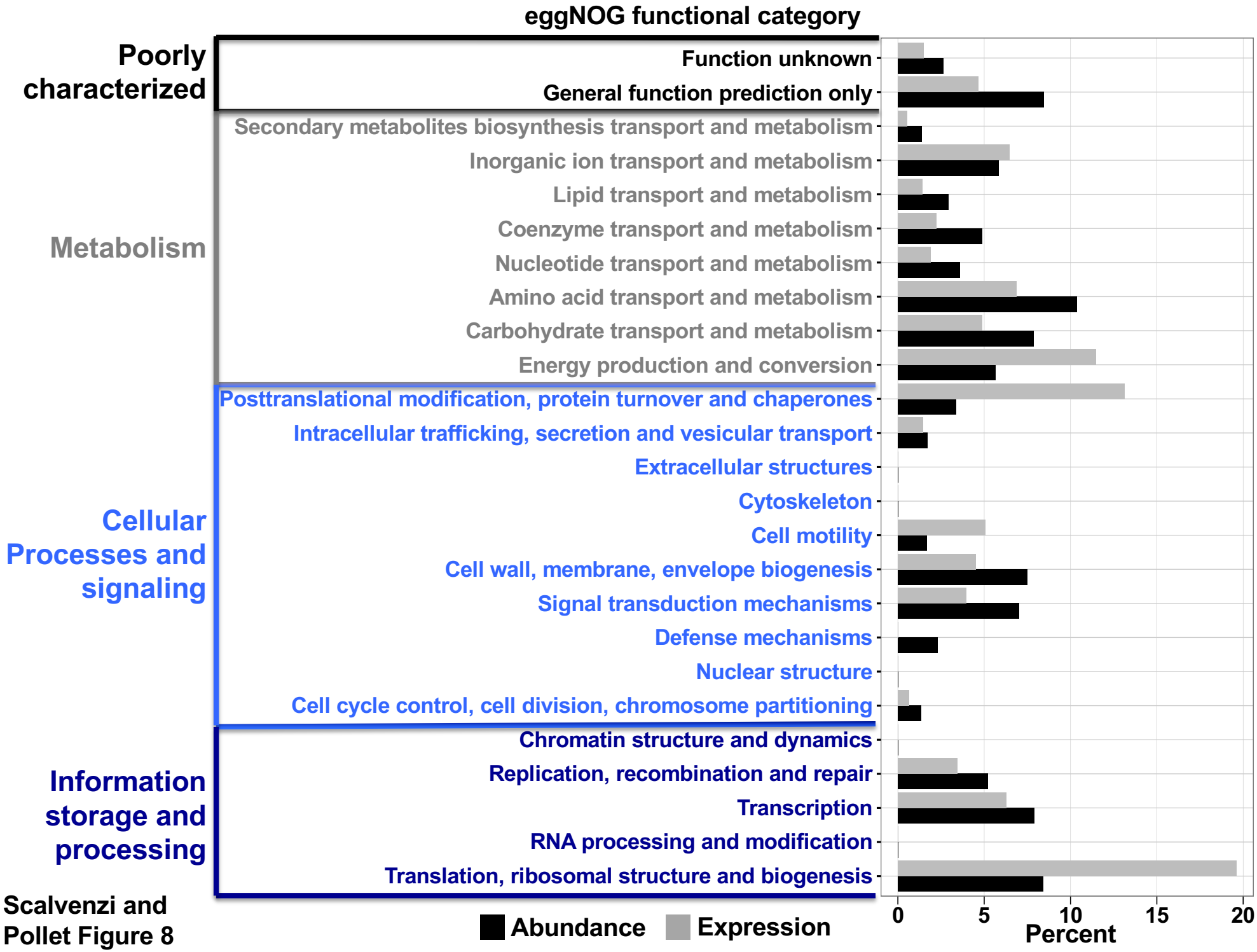

Scalvenzi and Pollet Figure 8

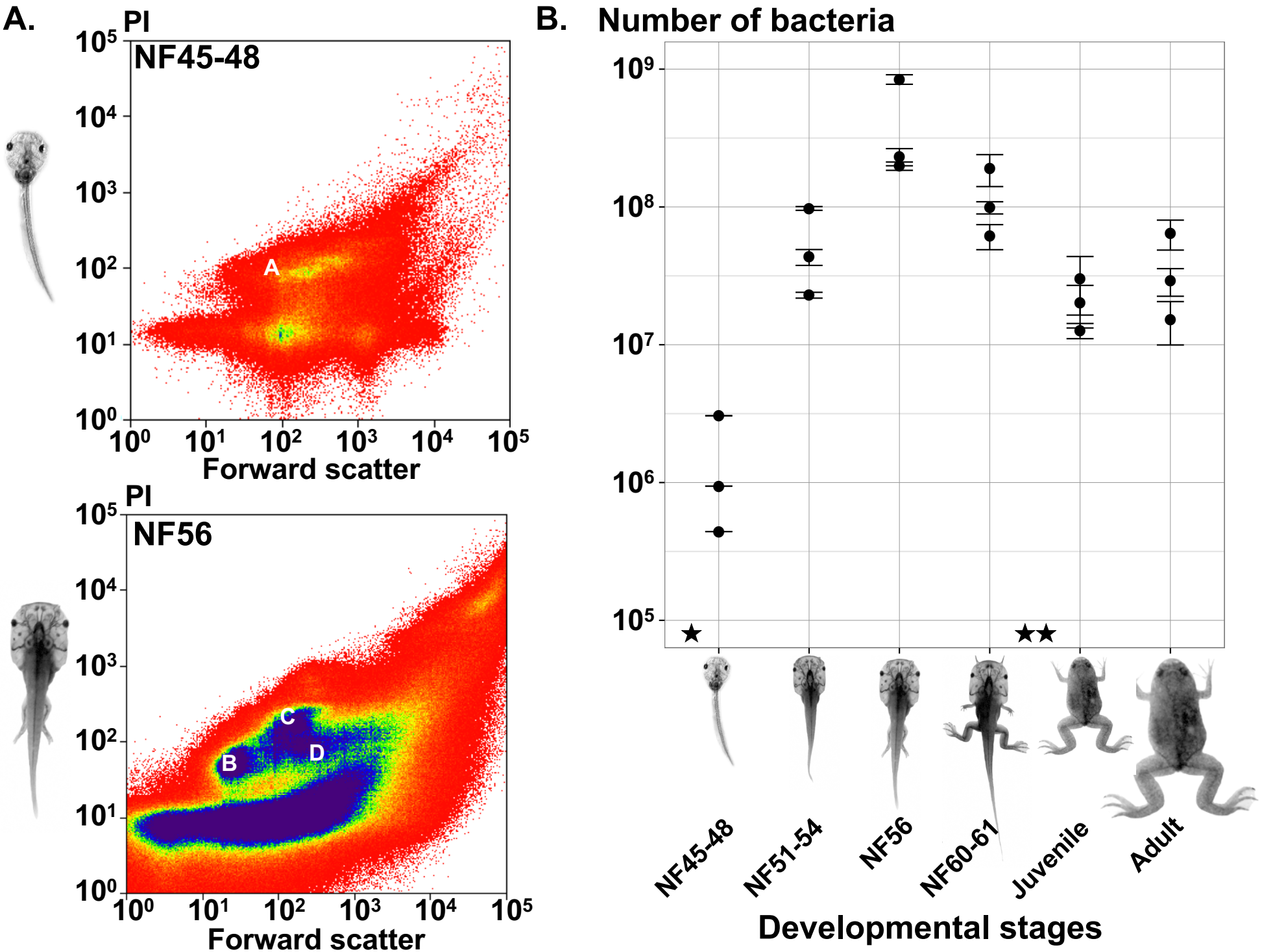
A.
PI
NF45-48
A
Forward scatter
PI
NF56
B
C
D
Forward scatter
B.
Number of bacteria
NF45-48
NF51-54
NF56
NF60-61
Juvenile
Adult
Developmental stages

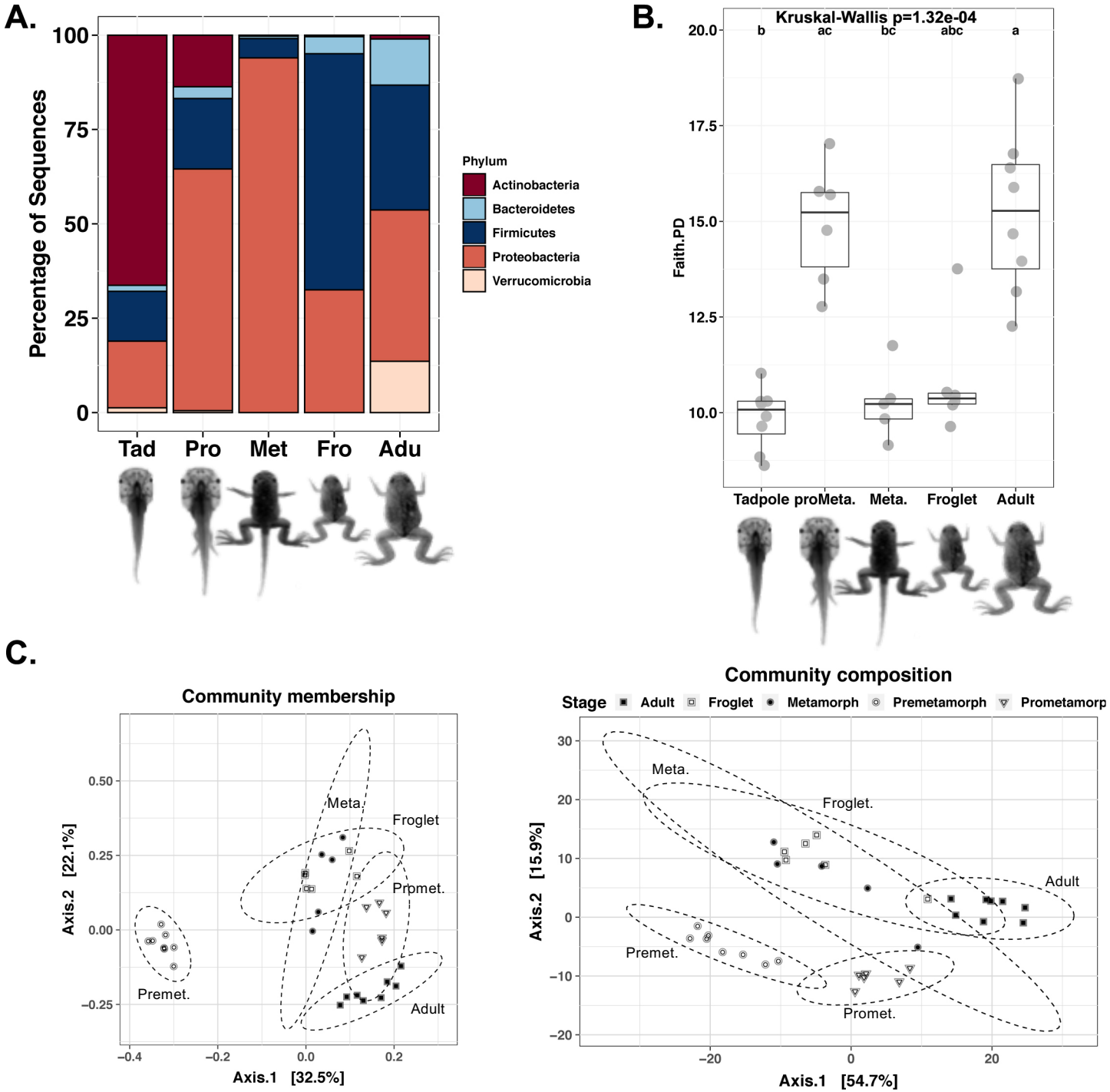
A.
Percentage of Sequences
100
75
50
25
0
Tad
Pro
Met
Fro
Adu
Phylum
Actinobacteria
Bacteroidetes
Firmicutes
Proteobacteria
Verrucomicrobia
B.
Kruskal-Wallis p=1.32e-04
b
ac
bc
abc
a
Faith.PD
20.0
17.5
15.0
12.5
10.0
Tadpole
proMeta.
Meta.
Froglet
Adult
C.
Community membership
Axis.2 [22.1%]
0.50
0.25
0.00
−0.25
−0.4
−0.2
0.0
0.2
Axis.1 [32.5%]
Meta.
Froglet
Prpmet.
Premet.
Adult
Community composition
Stage
Adult
Froglet
Metamorph
Premetamorph
Prometamorp
Axis.2 [15.9%]
30
20
10
0
−10
−20
−20
0
20
Axis.1 [54.7%]
Meta.
Froglet.
Adult
Premet.
Promet.

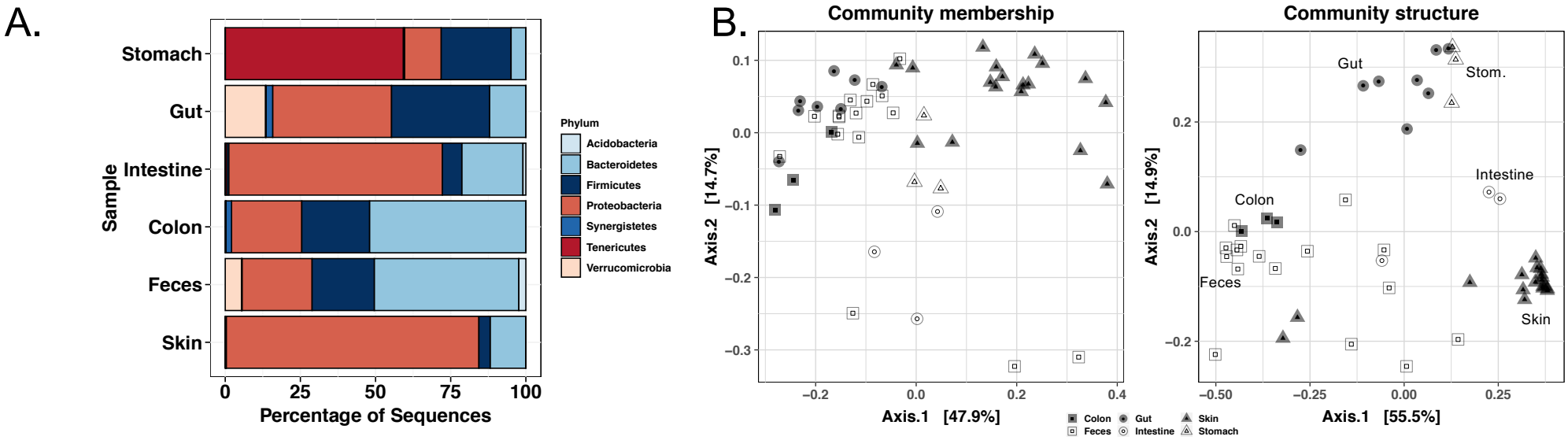
A.
Stomach
Gut
Intestine
Colon
Feces
Skin
Sample
0
25
50
75
100
Percentage of Sequences
Phylum
Acidobacteria
Bacteroidetes
Firmicutes
Proteobacteria
Synergistetes
Tenericutes
Verrucomicrobia
B.
Community membership
Community structure
Axis.2 [14.7%]
Axis.1 [47.9%]
Axis.2 [14.9%]
Axis.1 [55.5%]
Gut
Stom.
Intestine
Colon
Feces
Skin
Colon
Feces
Gut
Intestine
Skin
Stomach

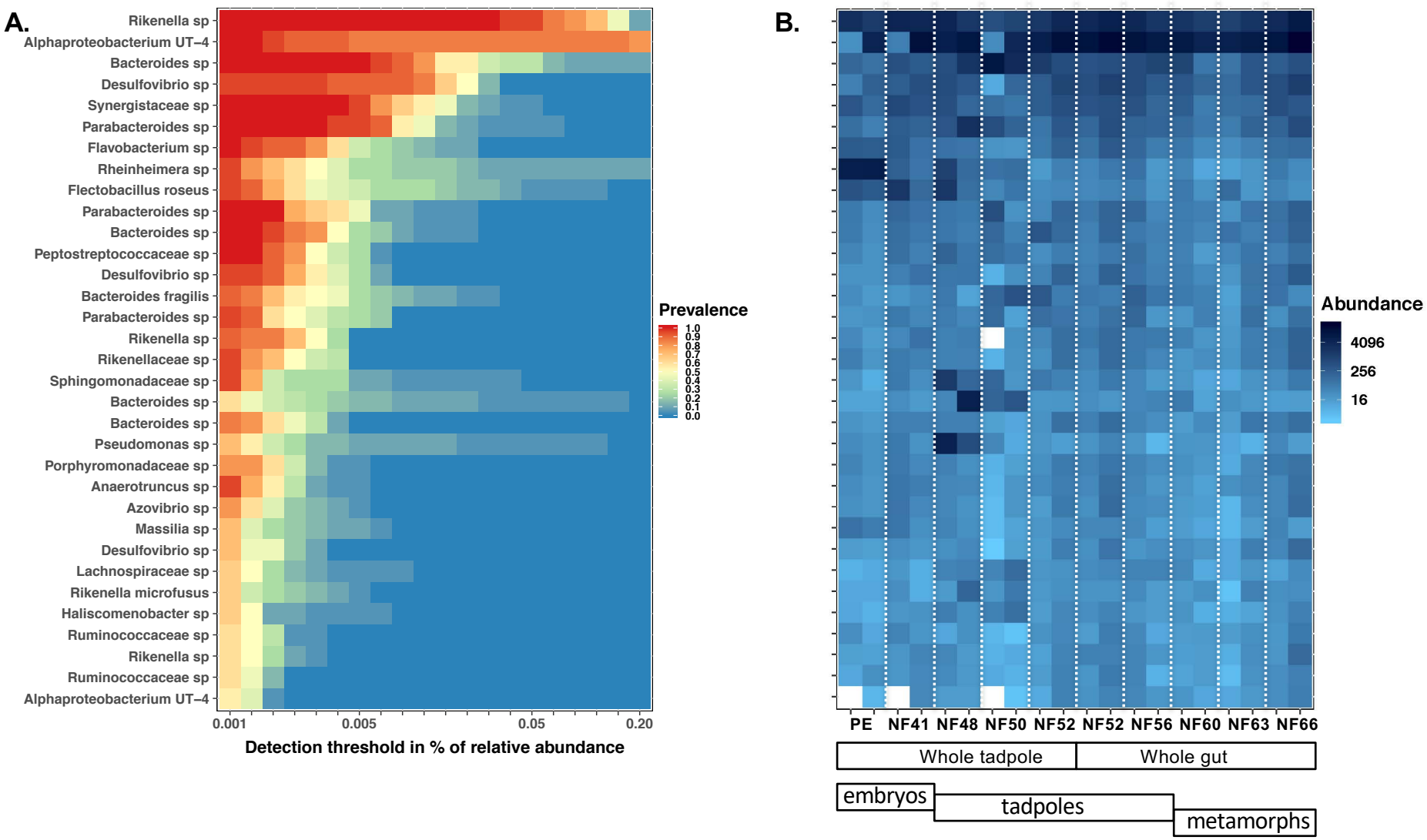
A.
Rikenella sp
Alphaproteobacterium UT−4
Bacteroides sp
Desulfovibrio sp
Synergistaceae sp
Parabacteroides sp
Flavobacterium sp
Rheinheimera sp
Flectobacillus roseus
Parabacteroides sp
Bacteroides sp
Peptostreptococcaceae sp
Desulfovibrio sp
Bacteroides fragilis
Parabacteroides sp
Rikenella sp
Rikenellaceae sp
Sphingomonadaceae sp
Bacteroides sp
Bacteroides sp
Pseudomonas sp
Porphyromonadaceae sp
Anaerotruncus sp
Azovibrio sp
Massilia sp
Desulfovibrio sp
Lachnospiraceae sp
Rikenella microfusus
Haliscomenobacter sp
Ruminococcaceae sp
Rikenella sp
Ruminococcaceae sp
Alphaproteobacterium UT−4
0.001
0.005
0.05
0.20
Detection threshold in % of relative abundance
Prevalence
1.0
0.9
0.8
0.7
0.6
0.5
0.4
0.3
0.2
0.1
0.0
B.
PE
NF41
NF48
NF50
NF52
NF52
NF56
NF60
NF63
NF66
Whole tadpole
Whole gut
embryos
tadpoles
metamorphs
Abundance
4096
256
16

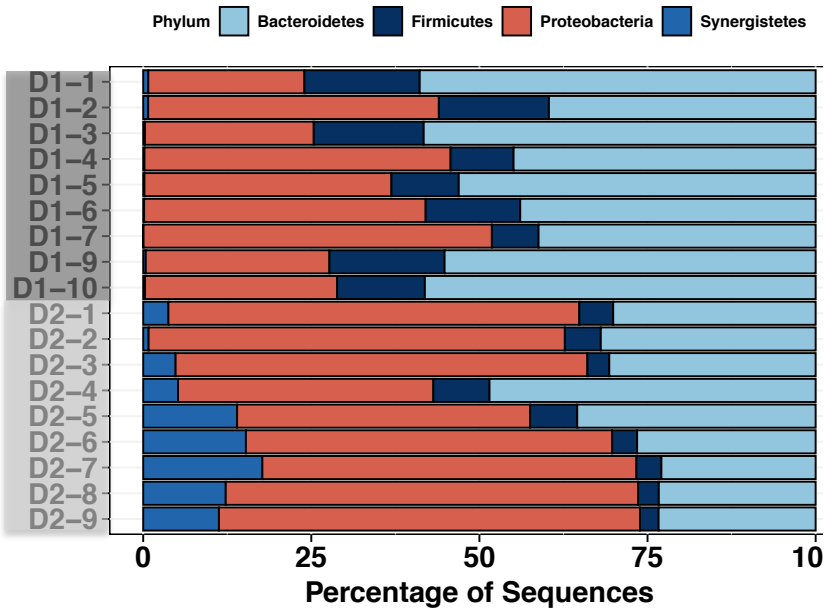
Phylum
Bacteroidetes
Firmicutes
Proteobacteria
Synergistetes
D1−1
D1−2
D1−3
D1−4
D1−5
D1−6
D1−7
D1−9
D1−10
D2−1
D2−2
D2−3
D2−4
D2−5
D2−6
D2−7
D2−8
D2−9
0
25
50
75
10
Percentage of Sequences

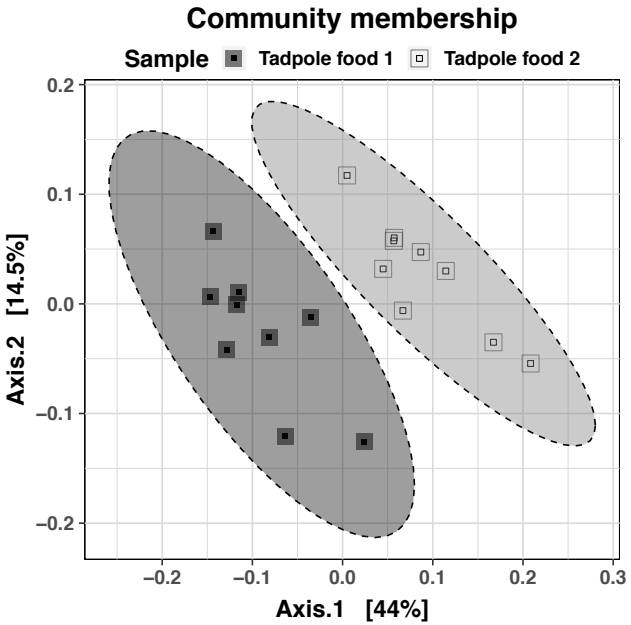
Community membership
Sample
Tadpole food 1
Tadpole food 2
Axis.2 [14.5%]
Axis.1 [44%]
0.2
0.1
0.0
−0.1
−0.2
−0.2
−0.1
0.0
0.1
0.2
0.3

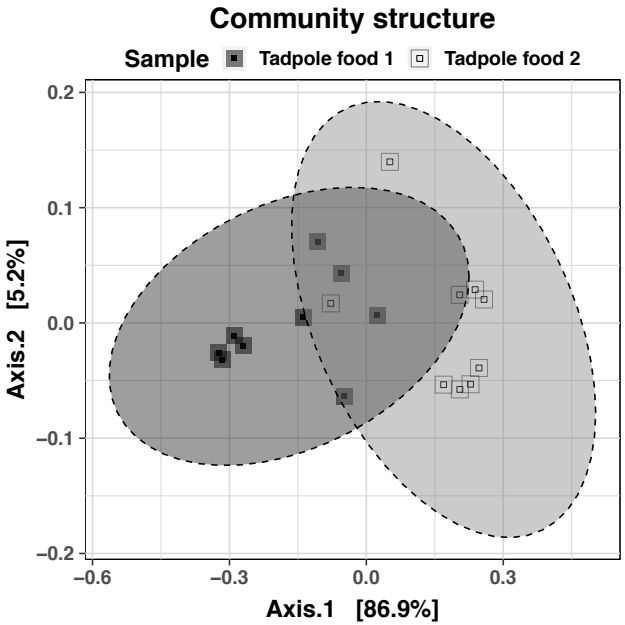
Community structure
Sample
Tadpole food 1
Tadpole food 2
Axis.2 [5.2%]
Axis.1 [86.9%]
0.2
0.1
0.0
−0.1
−0.2
−0.6
−0.3
0.0
0.3

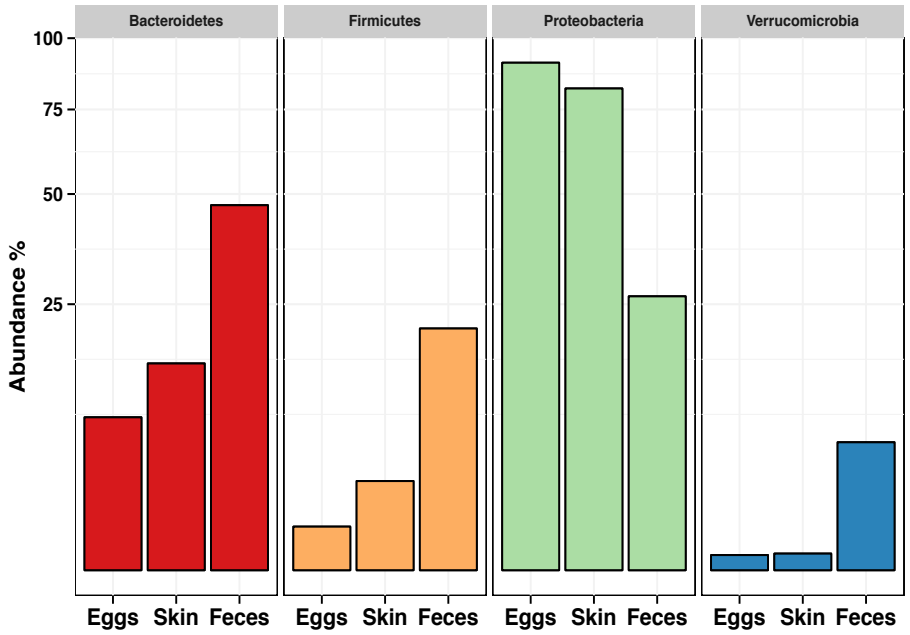
Bacteroidetes
Firmicutes
Proteobacteria
Verrucomicrobia
Abundance %
100
75
50
25
Eggs Skin Feces
Eggs Skin Feces
Eggs Skin Feces
Eggs Skin Feces

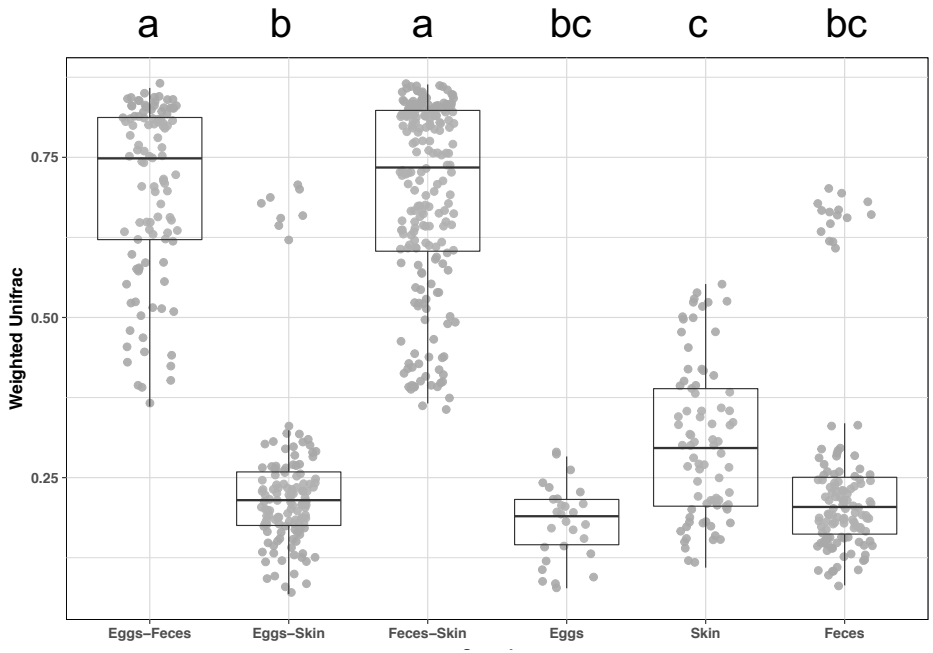
a b a bc c bc
Weighted Unifrac
0.75
0.50
0.25
Eggs–Feces
Eggs–Skin
Feces–Skin
Eggs
Skin
Feces

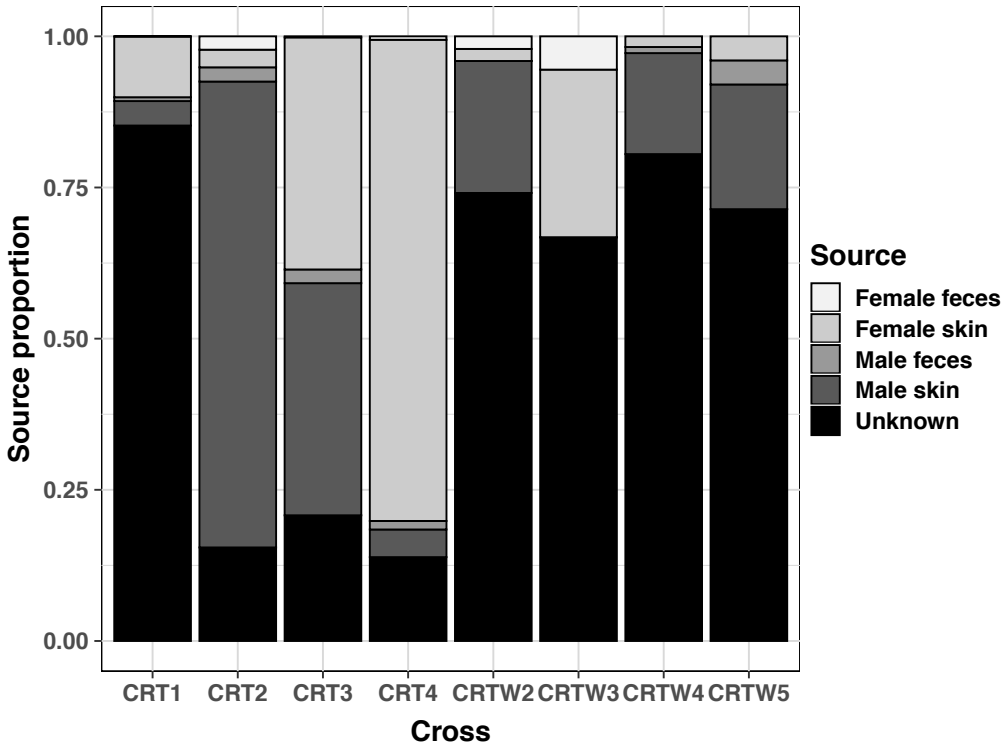
Source proportion
1.00
0.75
0.50
0.25
0.00
CRT1 CRT2 CRT3 CRT4 CRTW2 CRTW3 CRTW4 CRTW5
Cross
Source
Female feces
Female skin
Male feces
Male skin
Unknown

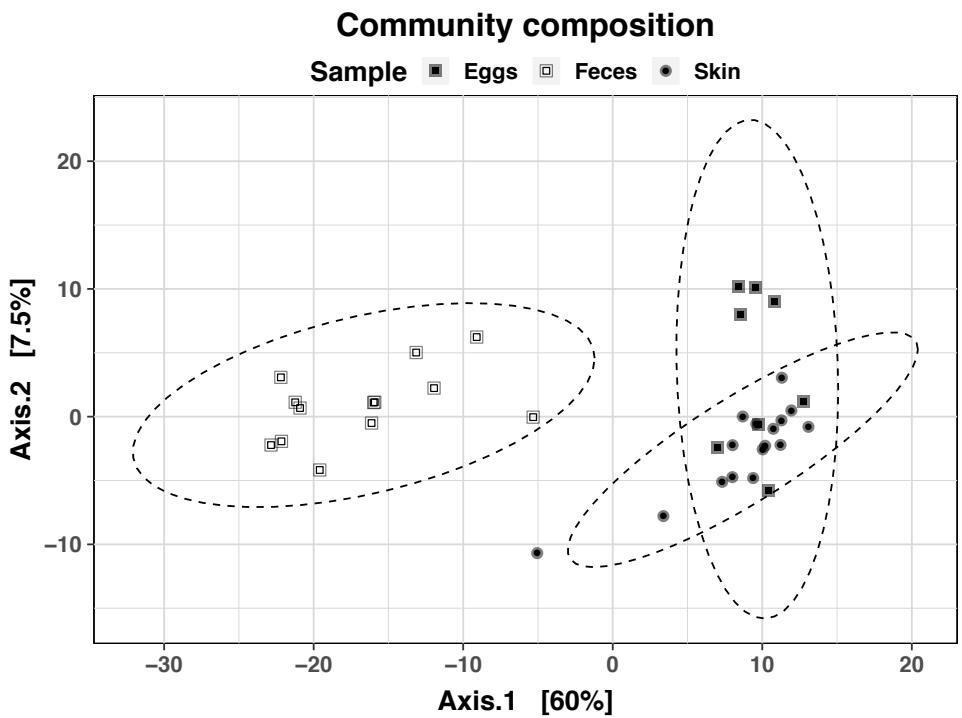
Community composition
Sample Eggs Feces Skin
Axis.2 [7.5%]
20
10
0
−10
−30 −20 −10 0 10 20
Axis.1 [60%]

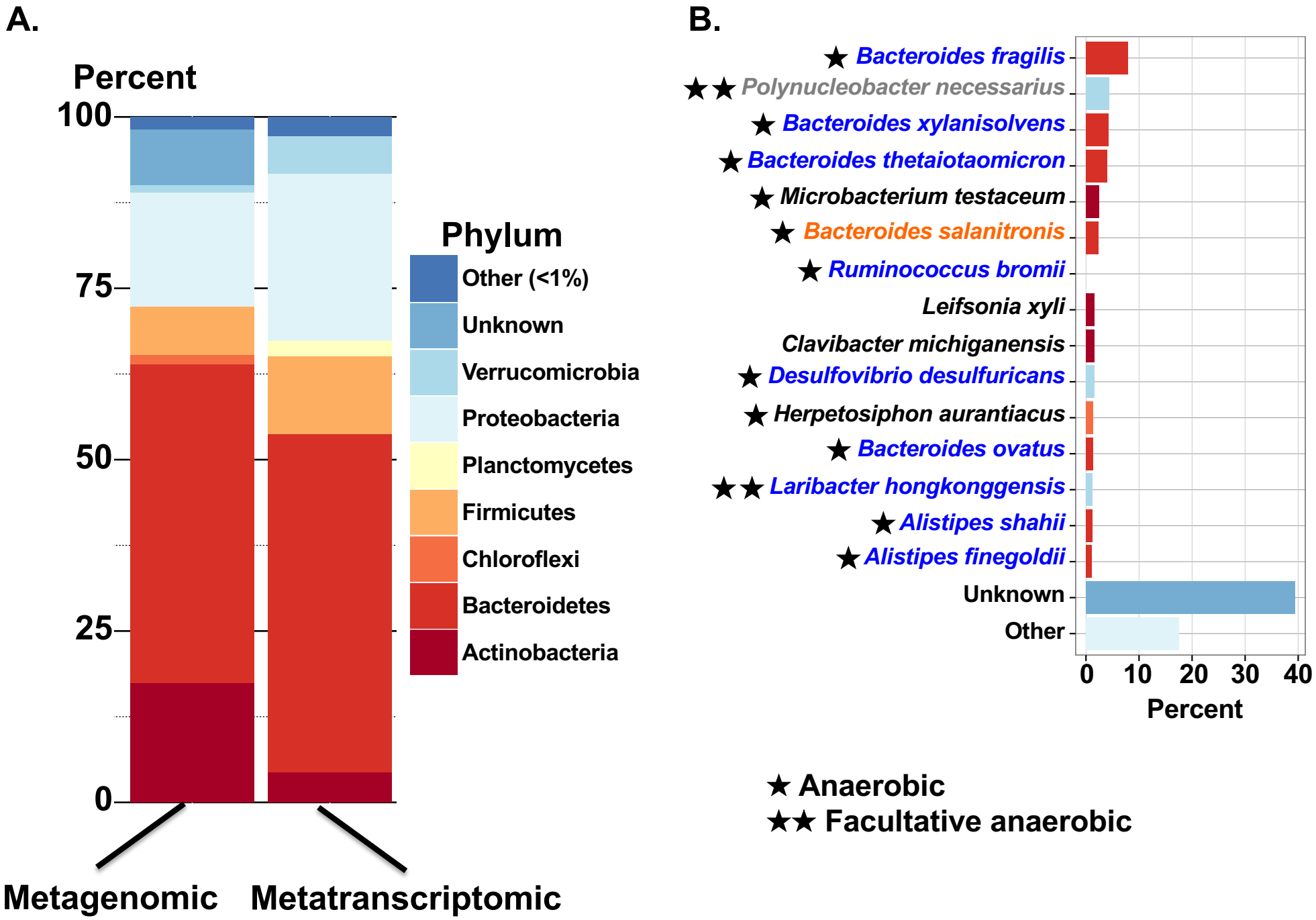
A.
Percent
100
75
50
25
0
Phylum
Other (<1%)
Unknown
Verrucomicrobia
Proteobacteria
Planctomycetes
Firmicutes
Chloroflexi
Bacteroidetes
Actinobacteria
Metagenomic
Metatranscriptomic
B.
Bacteroides fragilis
Polynucleobacter necessarius
Bacteroides xylanisolvens
Bacteroides thetaiotaomicron
Microbacterium testaceum
Bacteroides salanitronis
Ruminococcus bromii
Leifsonia xyli
Clavibacter michiganensis
Desulfovibrio desulfuricans
Herpetosiphon aurantiacus
Bacteroides ovatus
Laribacter hongkonggensis
Alistipes shahii
Alistipes finegoldii
Unknown
Other
0
10
20
30
40
Percent
Anaerobic
Facultative anaerobic

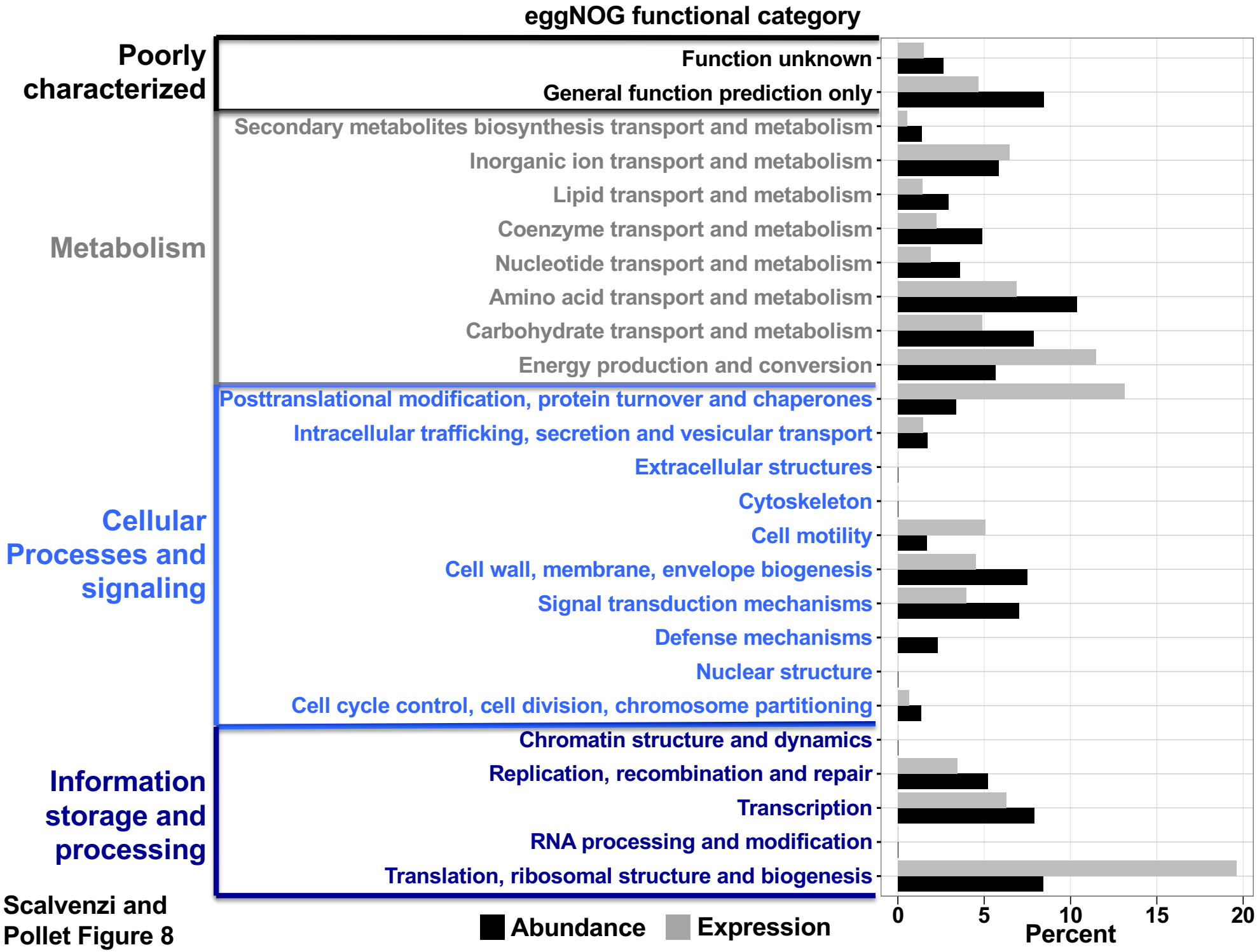

Scalvenzi and Pollet Figure 8